The Mechanics of Gross Moist Stability

David J. Raymond[1], Sharon L. Sessions[1], Adam H. Sobel[2] and Željka Fuchs[3]

[1] Physics Department and Geophysical Research Center, New Mexico Tech, Socorro, NM
[2] Departments of Applied Physics and Applied Mathematics and Earth and Environmental Sciences, Columbia University, New York, NY
[3] Physics Department, The University of Split, Split, Croatia

The gross moist stability relates the net lateral outflow of moist entropy or moist static energy from an atmospheric convective region to some measure of the strength of the convection in that region. If the gross moist stability can be predicted as a function of the local environmental conditions, then it becomes the key element in understanding how convection is controlled by the large-scale flow. This paper provides a guide to the various ways in which the gross moist stability is defined and the subtleties of its calculation from observations and models. Various theories for the determination of the gross moist stability are presented and its roles in current conceptual models for the tropical atmospheric circulation are analyzed. The possible effect of negative gross moist stability on the development and dynamics of tropical disturbances is currently of great interest.

1. Introduction

The gross moist stability (GMS) is the ratio of the vertically integrated horizontal divergence of some intensive quantity conserved in moist adiabatic processes and a measure of the strength of moist convection per unit area. Different authors have variously used moist static energy (Neelin and Held 1987, who originated the concept), equivalent potential temperature (Raymond 2000), and specific moist entropy (Raymond et al. 2007) as the conserved quantity. In addition, different measures of the convective strength have been used, including the convective mass flux per unit area (Neelin and Held 1987), the vertically integrated divergence of potential temperature flux (Fuchs and Raymond 2007), and the vertically integrated convergence of water vapor (Raymond et al. 2007). Though different in detail, these measures are all roughly equivalent in that the GMS is "a convenient way of summarizing our ignorance" (Neelin and Held 1987) about the relationship between convective forcing and the resulting response of convection.

The purpose of this paper is to develop a careful conceptual framework from which to view the GMS so that reliable measurements of this quantity can be defined. In addition the role of the GMS in various models and conceptual pictures of atmospheric convection and precipitation is discussed. Section 2 introduces basic definitions and motivates the work that follows. Section 3 develops the theoretical basis for calculating and measuring the GMS. Section 4 discusses the relationship of GMS to environmental conditions under

various hypotheses about the control of precipitation, particularly in tropical oceanic regions. The role of the GMS in current conceptual models of the large-scale tropical atmospheric flow is presented in section 5. Section 6 summarizes results and presents conclusions.

2. Motivation and definitions

To understand why the GMS is important in relating convection and convective forcing, let us consider the vertically integrated conservation equations for specific moist entropy s and total cloud water mixing ratio (vapor plus advected condensate) r in pressure coordinates, indicating the vertical pressure integral over the troposphere by square brackets:

$$\frac{\partial [s]}{\partial t} + \nabla \cdot [\mathbf{v}s] = F_s - R \qquad (2.1)$$

$$\frac{\partial [r]}{\partial t} + \nabla \cdot [\mathbf{v}r] = E - P. \qquad (2.2)$$

The quantity $\mathbf{v}$ is the horizontal wind, F_s is the moist entropy flux due to surface fluxes of heat and moisture, R is the pressure integral of the entropy sink due to radiative cooling, and E and P are the surface evaporation rate and the

To whom correspondence should be addressed.
David J. Raymond, Physics Department, New Mexico Tech, Socorro, NM 87801
raymond@kestrel.nmt.edu

precipitation rate respectively. In each case we have assumed that the pressure vertical velocity ω is zero at the surface and the tropopause so that $[\partial \omega s/\partial p] = 0$. Raymond et al. (2007) defined a particular version of the GMS, denoted the normalized gross moist stability (NGMS),

$$\Gamma_R = -\frac{T_R[\nabla\cdot(s\mathbf{v})]}{L[\nabla\cdot(r\mathbf{v})]} \qquad (2.3)$$

where $T_R = 300$ K is a constant reference temperature and L is the latent heat of condensation. The constants T_R and L are included to convert the entropy and total water mixing ratio divergences to energy units, thus making Γ_R dimensionless.

In a steady state, (2.1)-(2.3) imply that

$$P - E = \frac{T_R(F_s - R)}{L\Gamma_R}, \qquad (2.4)$$

which shows that the net precipitation $P - E$ is proportional to the "entropy forcing" $F_s - R$, and that the smaller the NGMS, the larger the constant of proportionality. The entropy forcing is larger for stronger surface heat and moisture fluxes, which over the ocean result from higher sea surface temperatures (SSTs) and stronger surface winds. Similarly, forcing is increased if radiative cooling is decreased by stratiform cloudiness in the middle and upper troposphere or an increase in humidity.

Given the above result, the determination of the NGMS as a function of environmental conditions becomes a prize worth pursuing. Raymond and Sessions (2007) and Raymond et al. (2007) used the cloud-resolving model of Raymond and Zeng (2005) to determine computationally the NGMS in steady state conditions for various imposed surface wind speeds and thermodynamic reference profiles. This model uses the weak temperature gradient (WTG) approximation to simulate the effect of embedding the modeled convection in a tropical environment. As the Coriolis force in the tropics is small, buoyancy anomalies are rapidly dispersed over a large area by gravity waves, leading to the WTG approximation that the mean virtual temperature profile in the convective domain is approximately the same as that in the surrounding environment. This is enforced by imposing horizontally averaged adiabatic cooling which just balances the averaged diabatic heating. The vertical velocity needed to generate this adiabatic cooling is called the weak temperature gradient vertical velocity. This vertical velocity profile is then used to advect moisture vertically in the convective domain. In addition, the horizontal velocity field required by mass continuity is used to entrain moisture from the surroundings where the horizontal flow is convergent. The characteristics of the surrounding air are defined by reference profiles of temperature and humidity.

Raymond et al. (2007) calculated Γ_R for convection in the WTG model for a range of imposed surface wind speeds and reference profiles of temperature and humidity obtained from a radiative-convective equilibrium calculation with the same model using 5 m s^{-1} imposed surface wind. Values of Γ_R in the range $0.4 - 0.6$ were obtained in this calculation. Raymond and Sessions (2007) extended these calculations to the case of reference profiles which are more moist and more stable (slightly warmer aloft and slightly cooler in the lower troposphere) than the radiative-convective equilibrium profile. Both of these reference profile modifications resulted in smaller values of Γ_R in the range $0.2 - 0.4$. Increased moisture and decreased instability are characteristic of convectively active areas of the tropics (Ramage 1971; Cho and Jenkins 1987; Williams et al. 1992), so these results suggest via (2.4) that more rain is produced for a given entropy forcing when these conditions hold.

Raymond and Fuchs (2009) divided the NGMS into two parts based on the identity

$$[\nabla\cdot(s\mathbf{v})] = [\mathbf{v}\cdot\nabla s] + [s\nabla\cdot\mathbf{v}]. \qquad (2.5)$$

Using the mass continuity equation in pressure coordinates

$$\nabla\cdot\mathbf{v} + \frac{\partial\omega}{\partial p} = 0 \qquad (2.6)$$

and integrating by parts in pressure, we have $[s\nabla\cdot\mathbf{v}] = [\omega(\partial s/\partial p)]$. Substitution into (2.3) results in $\Gamma_R = \Gamma_H + \Gamma_V$ (notation modified from Raymond et al. 2007) where

$$\Gamma_H = -\frac{T_R[\mathbf{v}\cdot\nabla s]}{L[\nabla\cdot(r\mathbf{v})]} \qquad (2.7)$$

and

$$\Gamma_V = -\frac{T_R[\omega(\partial s/\partial p)]}{L[\nabla\cdot(r\mathbf{v})]}. \qquad (2.8)$$

A similar division was made by Back and Bretherton (2006) in their study of the moist static energy budget in various regions over the Pacific Ocean. They referred to their analogs of Γ_H and Γ_V as the horizontal advection and vertical advection components, and found that both terms played significant roles in determining the moist static energy distribution. Raymond and Fuchs (2009) came to a similar conclusion for both the results of a toy tropical model and for the final analysis (FNL) produced by the National Centers for Environmental Prediction (NCEP). This is in contrast to the assumption of Neelin and Held (1987) that the horizontal advection term is not important.

Yu et al. (1998) estimated the pattern of GMS over the tropical regions using global analyses, concluding that it was modestly positive. However, these results must be viewed with some caution because the vertical pressure velocity profile was not obtained from observation, but from a version of the Betts-Miller convective parameterization (Betts 1986) which produces a vertical velocity structure consistent with the quasi-equilibrium hypothesis of

Emanuel et al. (1994). Since the term $\partial s/\partial p$ in the numerator of (2.8) changes sign with height, the vertical pressure integral $[\omega(\partial s/\partial p)]$ is a sensitive function of the form of $\omega(p)$ (e. g., Sobel 2007). There is no guarantee that the Betts-Miller (or any other) parameterization provides $\omega(p)$ with sufficient accuracy to produce a reliable estimate of $[\omega(\partial s/\partial p)]$. In addition, these authors included only the vertical advection part of the vertically integrated moist static energy flux divergence, ignoring their analog of Γ_H.

Back and Bretherton (2006) found that the vertical advection term tended to be negative in the east Pacific intertropical convergence zone and positive in the west Pacific warm pool, reflecting systematic differences in the vertical profiles of vertical velocity between the two regions. The horizontal advection term was positive in all rainy regions. The sum of the two tended to be uncertain in sign in the east Pacific, but positive in the west Pacific. Though more realistic than the study of Yu et al. (1998), the dependence on analysis vertical velocities nevertheless justifies some skepticism, given that global analyses inject model prejudices in data-sparse regions such as over tropical oceans.

Raymond and Fuchs (2009) calculated the NGMS in the western Pacific and eastern Indian Ocean using FNL data. As Back and Bretherton (2006) found, both the vertical and horizontal advection terms obtained from the FNL were positive in this region. However, the results obtained using the equatorial beta plane model of Raymond (2007) were quite different, with generally positive Γ_H and negative Γ_V averaged over the Indo-Pacific warm pool. It was hypothesized that the ability of the equatorial beta plane model to produce a robust Madden-Julian oscillation (MJO) was related to the negative values of Γ_V occurring in the model, i. e., to negative GMS as classically defined by Neelin and Held (1987). Support for this hypothesis comes from the FNL results, since the Global Forecast System (GFS) model of NCEP, which shares model physics with the FNL, produces an unrealistically weak MJO.

It is clear from the above comments that accurate measurement of the GMS over tropical oceans is a formidable problem, primarily because the vertically integrated vertical entropy (or moist static energy) advection is subject to large cancellations which leave a residual of uncertain sign. Sufficient sounding and airborne Doppler radar measurements were made in the Tropical Oceans Global Atmosphere Coupled Ocean Atmosphere Response Experiment (TOGA COARE; Webster and Lukas 1992) to estimate the numerator of Γ_V, i. e., $[\omega(\partial s/\partial p)]$ (López and Raymond 2005). Depending on the humidity of the troposphere, it was found that different convective regimes imported or exported moist entropy (or moist static energy); lower humidity environments tended to import these variables, whereas export occurred with higher humidity.

In addition, various measurement strategies highlight difficulties with how to define GMS. In particular, sparse sampling keeps us from knowing the wind and moist entropy structure in sufficient detail to calculate the NGMS at every point, and horizontal averaging inevitably must be introduced. The horizontal averages of $[\nabla\cdot(s\mathbf{v})]$ and $[\nabla\cdot(r\mathbf{v})]$ are individually amenable to measurement, since the average value of each can be obtained from measurements on the boundary of the averaging domain due to their form as divergences. However, the average of their ratio, which makes up the NGMS, is not amenable to this simplification. Thus, the "averaged" NGMS is best calculated by first averaging horizontally the vertically integrated horizontal flux divergences and then taking the ratio, and not the reverse.

Finally, different cumulus parameterization schemes in large-scale models may inadvertently result in values of the GMS which either preclude or over-emphasize certain processes. Adjusting these schemes to reproduce the actual patterns of GMS in the tropical environment should go a long way toward improving the quality of large-scale model forecasts in the tropics.

3. Theoretical basis

In this section we present various ways of calculating and measuring the NGMS. In most cases it is necessary to perform a certain amount of averaging to arrive at a stable estimate of the NGMS. However, averaging must be done carefully for the averaged quantity to make physical sense. Prescriptions for appropriate averaging are presented in this section. In addition, the advantages and disadvantages of various choices for the quasi-conserved thermodynamic quantity used in the definition of NGMS are discussed.

The source term on the right side of (2.1) includes all non-isentropic processes, the most prominent of which are the emission and absorption of thermal and solar radiation and the diffusion of heat and moisture into the atmosphere from the surface. However, an often-neglected component of this source term is the irreversible generation of entropy. Pauluis and Held (2002a) find that the primary mechanisms for this effect are irreversible phase changes and the diffusion of water vapor, with frictional dissipation playing a relatively small role.

The moist entropy is conserved by definition in slow, moist and dry adiabatic processes. The same cannot be said for the moist static energy (Madden and Robitaille 1970; Betts 1974). The reason is that the conservation of moist static energy depends on the hydrostatic approximation, which is not precisely valid when applied to a moving, accelerating parcel. Though deviations from hydrostatic balance may be small, the error accumulates. For steady flow, the moist Bernoulli function, which equals the moist static energy plus the specific parcel kinetic energy, is conserved. If the flow is not steady, then even this conservation principle is lost (López and Raymond 2005); we know of no general parcel conservation principle for the moist static energy or Bernoulli function.

In practice the non-conservation of moist static energy is relatively small in moist adiabatic motions in the atmosphere, and the difference between the moist entropy and moist static energy budgets is often negligible (López and Raymond 2005). However, in principle the non-conservative behavior of the moist entropy can be calculated in numerical models (Pauluis and Held 2002b), whereas the same cannot be said for the moist static energy. Thus, we mildly prefer to use the former in the definition of GMS, even though we do not attempt to calculate the irreversible generation of entropy here.

3.1. NGMS over a region

The NGMS when calculated from a snapshot of a single cumulus cloud is meaningless, as the flux divergences of entropy and water vapor on this scale are very noisy. In order to derive a stable quantity, significant averaging in space is necessary. As noted above, the only useful way to do this is to average separately over the numerator and denominator of Γ_R (2.3). For instance, if the over-bar indicates horizontal averaging over some spatial area A, then

$$\left[\overline{\nabla \cdot (s\mathbf{v})}\right] = \frac{1}{A}\left[\int_A \nabla \cdot (s\mathbf{v}) \, dA\right]$$
$$= \frac{1}{A}\left[\oint_{\partial A} s\mathbf{v}\cdot\mathbf{n} \, dl\right] \qquad (3.1)$$

where ∂A is the periphery of area A and $\mathbf{n}$ is the outward horizontal unit normal to ∂A. Equation (3.1) and its analog for water vapor can be used to define a meaningful average NGMS over the area A:

$$\bar{\Gamma}_R = -\left[T_R \oint_{\partial A} s\mathbf{v}\cdot\mathbf{n} \, dl\right] \Big/ \left[L \oint_{\partial A} r\mathbf{v}\cdot\mathbf{n} \, dl\right]. \qquad (3.2)$$

The virtue of this mode of averaging is that $\bar{\Gamma}_R$ requires knowledge of s, r, and $\mathbf{v}$ only along the periphery of the area, ∂A. Thus, $\bar{\Gamma}_R$ could be determined for a cluster of convection solely by dropsonde measurements around the cluster.

Note that Γ_H and Γ_V cannot be treated in the same way as Γ_R, as in neither case is the numerator in the form of a horizontal divergence. However, s can be split into an average value around the periphery at each pressure level $\tilde{s}(p)$ and a perturbation $s*$ from this value. Substituting this into (3.2) results in a corresponding split of $\bar{\Gamma}_R$ into symmetric and asymmetric parts, $\bar{\Gamma}_R = \bar{\Gamma}_S + \bar{\Gamma}_A$. Using the mass continuity equation in pressure coordinates (2.6), reverting to the area integral, and integrating by parts in pressure, we have

$$\bar{\Gamma}_S = -AT_R\left[\bar{\omega}\frac{\partial \tilde{s}}{\partial p}\right] \Big/ \left[L \oint_{\partial A} r\mathbf{v}\cdot\mathbf{n} \, dl\right] \qquad (3.3)$$

where $\bar{\omega}$ is the pressure vertical velocity averaged over the area A. The quantity $\partial\bar{\omega}/\partial p$ is obtained by applying the divergence theorem to the mass continuity equation:

$$\frac{\partial\bar{\omega}}{\partial p} = -\frac{1}{A}\oint_{\partial A} \mathbf{v}\cdot\mathbf{n} \, dl. \qquad (3.4)$$

Thus, even though $\bar{\omega}$ is an average over A, it is derived from values of the horizontal velocity on the periphery ∂A. The quantity $\bar{\Gamma}_S$ resembles the unaveraged vertical advection component of NGMS, Γ_V (2.8). It is therefore similar, but not identical, to the original definition of GMS, but is in a form which can be derived from measurements solely on the periphery of a convective system.

The other component of $\bar{\Gamma}_R$ is simpler,

$$\bar{\Gamma}_A = -\left[T_R \oint_{\partial A} s*\mathbf{v}\cdot\mathbf{n} \, dl\right] \Big/ \left[L \oint_{\partial A} r\mathbf{v}\cdot\mathbf{n} \, dl\right]. \qquad (3.5)$$

The quantity $\bar{\Gamma}_A$ is only non-zero when the convection inside area A is not statistically axisymmetric. Lack of axisymmetry is typically the result of non-zero wind relative to the area A containing the convection. This wind blowing through the convective region is likely to entrain higher entropy air from the convection, resulting in negative $s*$ on the inflow side and positive $s*$ on the outflow side. It thus represents the effects of ventilation, which in many circumstances makes it similar to the unaveraged horizontal advection term Γ_H.

The quantities $\bar{\Gamma}_S$ and $\bar{\Gamma}_A$ are useful for determining the properties of isolated disturbances such as tropical cyclones. Since such disturbances are generally moving, it is appropriate to define $\mathbf{v}$ as the wind field relative to the reference frame moving with the disturbance. Marín et al. (2009) used this technique to monitor the characteristics of tropical storms as represented by the NCEP Global Forecast System (GFS) model.

3.2. NGMS in models

In large-scale models the wind and thermodynamic fields are effectively low-pass filtered by the finite grid resolution. Defining this low pass filtering by angle brackets, the entropy and velocity can be split into filtered and residual parts $s = <s> + s'$ and $\mathbf{v} = <\mathbf{v}> + \mathbf{v}'$ and the filtered entropy flux divergence can be written in the usual way, $<\nabla \cdot (s\mathbf{v})> = \nabla \cdot (<s> <\mathbf{v}>) + \nabla \cdot <s'\mathbf{v}'>$, where we make the Reynolds decomposition assumptions that $<s'<\mathbf{v}>> = 0$, etc. It is not obvious in the real world that one can neglect $\nabla \cdot <s'\mathbf{v}'>$. However in models, terms like this are almost universally ignored, so they must be excluded from model diagnostics as well. It is thus appropriate to drop the angle bracket notation and consider s, r, and $\mathbf{v}$ to be implicitly smoothed to the grid scale.

Spatial averaging of $\left[\nabla \cdot (s\mathbf{v})\right]$ in this case has an interpretation in terms of lateral entropy fluxes in and out of the averaging domain, as discussed in section 3.1. However, as noted in that section, spatial averages of the individual components of the vertically integrated flux

divergence as defined by (2.5) do not. Over all, it is probably more physically justified to employ the procedure outlined in section 3.1 when spatial averaging is applied. However, if the averaging is done over a relatively homogeneous region, then the difference between the two methods is likely to be small, since the average of moist entropy over the periphery of a region $\tilde{s}$ in (3.3) is not likely to be too different from the average of s over the region itself in (2.8).

3.3. Averaging over time

An alternate form of the above Reynolds decomposition which should be valid for both observational data and models is to take the averaging to be over time. In this case the total moist entropy flux divergence is considered to consist of a part constructed solely from the timemean variables plus a part constructed from the fluctuating parts of the velocity and entropy fields. In time averaging the latter generally cannot be ignored. However, to the extent that the Reynolds decomposition is valid, these parts of the entropy flux divergence can be considered independently.

4. The GMS and environmental conditions

The GMS becomes an interesting tool only if it is a knowable function of environmental conditions. In this section various hypotheses for the behavior of the GMS (and the NGMS) are explored. In addition, the differences between the GMS in steady and non-steady conditions are indicated. Finally, the co-evolution of GMS and precipitation rate and the possible development of multiple equilibria given the same external forcing are discussed.

4.1. Neelin-Held (1987) model

Neelin and Held (1987) in their seminal paper on the GMS postulated that the low level convergence, and hence the convection and precipitation in their two-layer model, was proportional to the moist static energy forcing (surface minus tropopause moist static energy flux) divided by their original definition of GMS, which they expressed as the upper tropospheric minus the lower tropospheric moist static energy. The SST governs the lower tropospheric moist static energy in their model on the assumption of fixed sea-air temperature difference and fixed relative humidity. Their postulate was used to explain the sensitivity of convection to SST, particularly at the upper end of the SST range. The Neelin-Held (1987) postulate may have some continuing value in explaining tropical precipitation climatology, but it fails on a day-to-day basis due to its inability to account for the high observed variability in convection and precipitation over regions of elevated SST.

4.2. Raymond (2000) hypothesis

Raymond's (2000) hypothesis that precipitation over warm tropical oceans is a function solely of the column relative humidity or saturation fraction (precipitable water divided by saturated precipitable water) provides an alternative model for the forcing of precipitation. Given this hypothesis, the problem of precipitation forcing reduces to understanding the laws governing saturation fraction.

At the time, Raymond's hypothesis was little more than a guess, but subsequent results provide significant support for the hypothesis over space and time scales of order 100 km and a large fraction of a day. Various cloud-resolving models show a strong sensitivity of average precipitation rate to tropospheric humidity (Lucas et al. 2000; Derbyshire et al. 2004; Raymond and Zeng 2005) as do satellite observations using passive microwave imagery (Bretherton et al. 2004; Peters and Neelin 2006) and conventional sounding and radar data (Raymond et al. 2007; see figure 1). The cloud resolving model results of Raymond and Zeng (2005) are in reasonable agreement with these observations, as the curve in figure 1 shows. (The non-zero precipitation rates inferred for soundings with low saturation fraction are spurious and are due to incorrect conversion of infrared brightness temperature to precipitation rate with the simple formula used by Raymond et al. 2003.)

Back and Bretherton (2005) showed that saturation fraction is not the only factor governing precipitation. In their study, for particular saturation fraction values, precipitation rate increases with increasing surface wind speeds and associated surface heat and moisture fluxes. Generally, we expect convection also to have some dependence on measures of column stability such as convective available
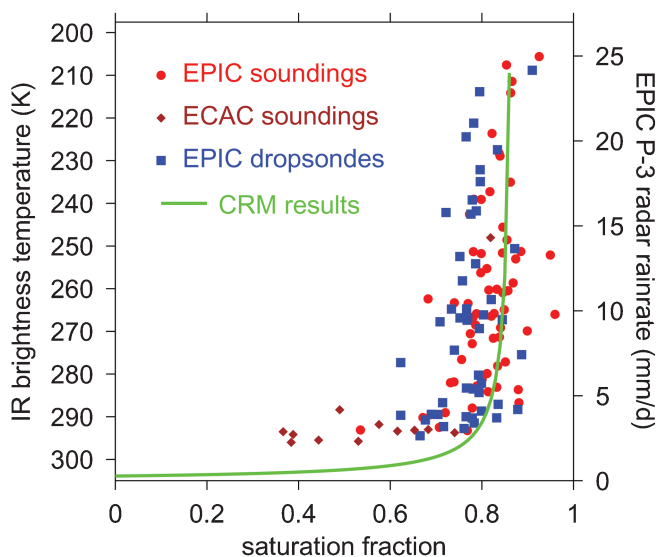

Figure 1. Infrared brightness temperature and inferred precipitation rate versus saturation fraction computed from soundings in the east Pacific and the southwest Caribbean. Precipitation rate was inferred from a calibration of satellite infrared brightness temperatures using airborne meteorological radar data. The cloud resolving model curve is a fit to the results of Raymond and Zeng (2005). Adapted from Raymond et al. (2007).

potential energy and convective inhibition, as it does in typical convective parameterizations used in climate models. However, at least for the purposes of first order qualitative theories of large-scale variations of deep convection over warm tropical oceans, it may be fair to say that the variation in saturation fraction is the dominant contributor to the variation in precipitation rate.

The steepness of the relationship between precipitation rate and saturation fraction in the cloud-resolving model can be related to the dependence of both rainfall and saturation fraction on the external control parameters which determine the occurrence and intensity of convection in the model. SST and surface wind speed are typically used as such control parameters in WTG simulations (Raymond and Zeng 2005; Raymond et al. 2007). For fixed SST, we therefore write

$$\frac{dP}{dS} = \frac{dP/dU}{dS/dU} \tag{4.1}$$

where P is the precipitation rate, S is the saturation fraction, and U is the boundary layer wind. As figure 2 shows, in this model the saturation fraction increases with imposed wind up to winds of order 7 m s^{-1} and then approaches an
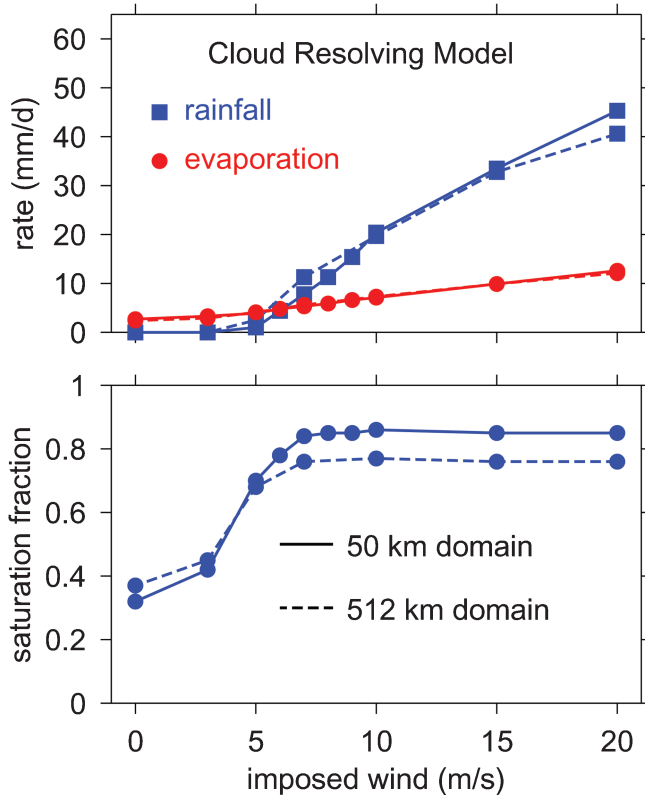
asymptotic value near 0.87 for higher wind speeds. As a result dS/dU approaches zero, which means that dP/dS becomes very large, as illustrated in figure 3. In essence, the model is maintained in a state of conditional instability by the WTG condition and the increase in saturation fraction reduces the threshold for the initiation of convection, allowing almost arbitrarily large precipitation rates to occur, which in turn acts to limit the further growth of saturation fraction. The agreement between the CRM and observation in figure 1 suggests that the asymptotic limit on saturation fraction occurs in the natural world as well. (See also the work of Peters and Neelin 2006.)

Raymond's (2000) analysis depends on a knowledge of the GMS. Raymond et al. (2007) and Raymond and Sessions (2007) showed how to infer the NGMS from a cloud resolving numerical model run in weak temperature gradient mode (Sobel and Bretherton 2000; Sobel et al. 2001; Raymond and Zeng 2005). However, these model results provide little physical insight into the processes governing the NGMS. The boundary layer quasi-equilibrium (BLQ) model of Raymond (1995; see also Emanuel 1995) casts light on this problem.

4.3. Boundary layer quasi-equilibrium

In Raymond (1995) and Emanuel (1995) the boundary layer is maintained on the verge of convection by a balance between surface latent and sensible heat fluxes which increase the moist entropy of the boundary layer on one hand, and convective downdrafts, clear air entrainment into
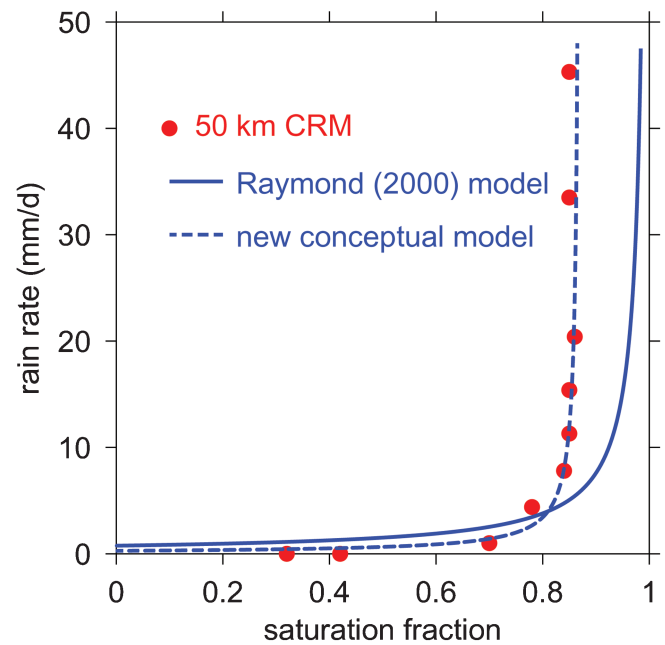

Figure 2. Results of WTG calculations with cloud resolving model on 50 km and 512 km domains. (a) Precipitation and evaporation rate in equilibrium as a function of imposed wind speed. (b) Mean equilibrium saturation fraction in model domain as a function of imposed wind speed. Adapted from Raymond (2007).

Figure 3. Precipitation rate as a function of saturation fraction in Raymond (2000) conceptual model (solid line), the Raymond and Zeng (2005) CRM results (bullets), and a new conceptual model adjusted to fit the Raymond-Zeng results (dashed line; also shown in figure 1). Adapted from Raymond et al. (2007).

the boundary layer, and direct radiative cooling on the other hand, which decrease it. The downdraft flux, thus specified, implies a certain updraft flux, convective coverage, and mean precipitation rate, given a cloud physical model of how these quantities are related. BLQ thus in principle contains all the ingredients needed to determine the GMS in any of its many forms.

BLQ analyzes the conservation equation for the moist entropy perturbation $s - s_b$

$$\frac{\partial [s - s_b]_B}{\partial t} + \nabla \cdot [(s - s_b)\mathbf{v}]_B$$
$$+ \left[\frac{\partial (s - s_b)\omega}{\partial p}\right]_B = F_s - R_b \qquad (4.2)$$

integrated over a control volume of the planetary boundary layer (PBL) as illustrated in figure 4. The quantity s_b is a constant reference specific moist entropy characteristic of the planetary boundary layer (PBL) in our idealized picture, F_s is the surface flux of specific entropy associated with surface heat and moisture fluxes, and R_b is the pressure integral of radiative cooling in the PBL. The square brackets with a subscripted B indicate integration in pressure over the PBL.

In this idealized picture both the air flowing laterally into the control volume and the air rising out of the top in convective updrafts have $s \approx s_b$. Thus, integrating (4.2) over the control volume and applying the divergence theorem results in approximately zero contribution from the lateral inflow and the updraft outflow. Observations in the east Pacific intertropical convergence zone indicate that this is not a bad approximation (Raymond et al. 2006).

The quasi-equilibrium assumption of BLQ requires that the time derivative in (4.2) be dropped. Thus, we end up
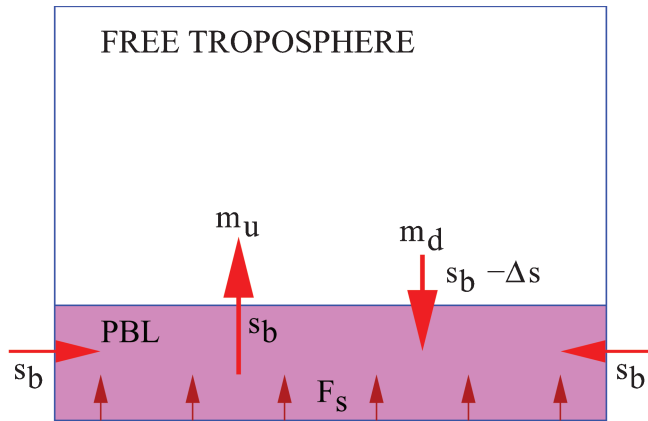

FREE TROPOSPHERE

m_u m_d $s_b - \Delta s$

PBL s_b

s_b s_b

F_s

Figure 4. Sketch of mass flows and entropy transports in boundary layer quasi-equilibrium. The updraft and downdraft mass fluxes are m_u and m_d. The surface entropy flux is F_s. The planetary boundary layer (PBL) has entropy approximately equal to s_b and laterally inflowing air and outflowing updraft air both carry this specific entropy value as well. Downdraft air has specific entropy $s_b - \Delta s$.

with a balance primarily between convective downdrafts and surface moist entropy fluxes, ignoring the contributions of radiation in the PBL and clear air entrainment from above the PBL. These terms must be included in a quantitatively accurate accounting for the moist entropy budget, but are relatively minor contributors in convectively active regions.

The updraft and downdraft mass fluxes through the top of the PBL are m_u and m_d, and they are assumed to vary in proportion,

$$m_d = a m_u \qquad (4.3)$$

with a proportionality factor a which depends on the response of the convection to the prevailing environment. The entropy flux out of the boundary layer due to downdrafts entering the PBL is $m_d \Delta s$ where $s_b - \Delta s$ is the specific entropy of downdraft air. Clear air entrainment into the boundary layer is also included in the term $m_d \Delta s$. We equate this to the surface moist entropy flux F_s according to the above approximations and infer that

$$m_u = m_d/a = F_s/(a\Delta s). \qquad (4.4)$$

The flux of moisture out of the top of the boundary layer is $m_u r_b - m_d r_d$ where r_b is the mixing ratio in the PBL and $r_d = r_b - \Delta r$ is the mixing ratio of air entering the PBL from above in downdrafts. If the temperature anomalies in the updraft and downdraft are not large, as is typical above the surface, then the mixing ratio deficit of air entering the boundary layer is related directly to the moist entropy deficit $\Delta r \approx T_R \Delta s / L$ and the precipitation rate P can be written

$$P = \varepsilon(m r_b + m_d T_R \Delta s / L) \qquad (4.5)$$

where the net mass flux $m = m_u - m_d = m_d(1 - a)/a$ and where we have made the assumption that the precipitation rate is proportional to the moisture flux upward out of the boundary layer. The constant of proportionality ε is a kind of precipitation efficiency. Since moisture can be converged into the column above the PBL, it is possible that $\varepsilon > 1$. However, ε is less if some fraction of the moisture converged at low levels is not rained out, but is ejected laterally from the column as vapor or advected condensate. As the precipitation rate is observed to be a strong function of the saturation fraction S, we incorporate a large part of this dependence into ε by making $\varepsilon(S)$ asymptote rapidly toward zero for saturation fractions less than, say, 0.7 (see figure 3).

In a steady state we use (2.4) to infer the NGMS,

$$\Gamma_R = \frac{T_R(F_s - R)}{L(P - E)}. \qquad (4.6)$$

Over warm tropical oceans the latent heat flux dominates the sensible heat flux, so that

$$LE \approx T_R F_s. \qquad (4.7)$$

We define the variable

$$\sigma = \frac{T_R \Delta s}{L r_b} \qquad (4.8)$$

as a dimensionless downdraft entropy deficit and note that $\sigma \ll 1$ since the mixing ratio deficit $\Delta r = T_R \Delta s / L$ is typically much less than the PBL mixing ratio r_b.

Putting all of this together results in an estimate for the NGMS in terms of the dimensionless parameters a, $\varepsilon(S)$, σ, and R/F_s,

$$\Gamma_R = \frac{(1 - R/F_s) a \sigma}{\varepsilon(S)(1 - a + a\sigma) - a\sigma}. \qquad (4.9)$$

We note several features of this equation:

1. Downdrafts are key to the control of convection in BLQ, and eliminating the downward transport of low entropy air into the PBL by setting either the downdraft-updraft mass flux ratio a or the dimensionless downdraft entropy deficit σ to zero results in $\Gamma_R = 0$.

2. Two regimes exist, one with $F_s < R$ the other with $F_s > R$. The former corresponds to negative entropy forcing of the troposphere and requires the lateral import of entropy in the steady state. The latter regime corresponds to positive entropy forcing and exports entropy laterally. Negative entropy forcing generally corresponds to weak surface winds and corresponding weak surface fluxes, while positive entropy forcing occurs for strong surface winds.

3. Since a stable equilibrium state generally requires $\Gamma_R > 0$, a steady weak surface wind regime requires the denominator of (4.9) to be negative, i. e., $\varepsilon < a\sigma/(1 - a + a\sigma)$, while the reverse condition holds for the strong surface wind regime. Thus, stability requires low precipitation efficiency for light winds and high precipitation efficiency for strong winds. The exception to this rule occurs for the case of a dry troposphere with no rain and strong winds. In this case $\varepsilon = 0$ and $\Gamma_R = -(1 - R/F_s) < 0$ as discussed previously.

Recent work suggests that BLQ does not hold for certain rapidly moving wave disturbances such as convectively coupled equatorial Kelvin waves. Raymond and Fuchs (2007) showed that modulation of convection in such modes can be explained by wave-related adiabatic lifting of the capping layer just above the PBL. Furthermore, Roundy and Frank (2004) showed that relative to other types of tropical disturbances, the Kelvin wave signal is much weaker in precipitable water than in outgoing long-wave radiation. This points to an alternative convective forcing mechanism for these waves, which does not depend as strongly on saturation fraction.

4.4. Transient flows

If the precipitation rate and the tropospheric humidity are changing with time, then we need to include the possibility
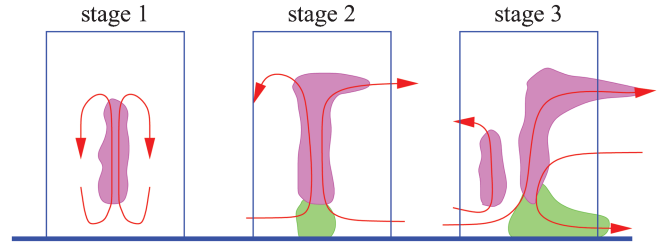

Figure 5. Schematic illustration of the stages of evolution of the onset of convection in a control volume. See text for further explanation.

that the NGMS is also changing. Figure 5 illustrates how the flows and transports respond to the step function development of convection in a control volume such as that considered in section 3.1. In stage 1 the compensating subsidence from the newly formed convection occurs locally, and no signal reaches the walls of the control volume. In stage 2, the compensating subsidence signal, which moves rapidly outward at the speed of gravity waves with vertical scale equal to that of the convection (Bretherton and Smolarkiewicz 1989), has passed through the walls of the control volume. This means that the lateral flows associated with convective convergence and divergence now penetrate the control volume walls. However, the actual air detrained by the convection, which typically moves outward much less rapidly than the gravity waves, has yet to reach the walls. This air may come from the anvil outflow, boundary layer downdraft outflows, or mid-level detrainment (see e. g., Raymond and Blyth 1986). Finally, in stage 3 both the convergent and divergent flows and the material outflows from the convection have reached the walls and the interior of the control volume approaches a statistically steady state.

The above picture is over simplified in some respects. The gravity waves emitted laterally by convection exhibit a vertical spectrum with a mixture of deep and shallow scales. Since the hydrostatic gravity wave propagation speed is proportional to the vertical scale, the wave response at the control volume boundary will only gradually come to reflect the true vertical profile of convergence and divergence in the convection, and the propagation speed of the waves with shorter vertical wavelengths may be less than the speed with which material outflows advance. This may be particularly true in a sheared environment where the environmental flow relative to the convection can transport convectively modified air rapidly away from the convective region. This picture nevertheless provides a rough guide to what happens under many circumstances, especially for tropical convection where the shear is often small.

In stage 2 the vertical profile of entropy averaged around the periphery of the control volume of interest $\tilde{s}(p)$ is that characteristic of the flow previous to the change in convection except for the possible effects vertical displacements due to the passing subsidence wave, while $\bar{\omega}(p)$ represents the mean pressure vertical velocity profile after the change.
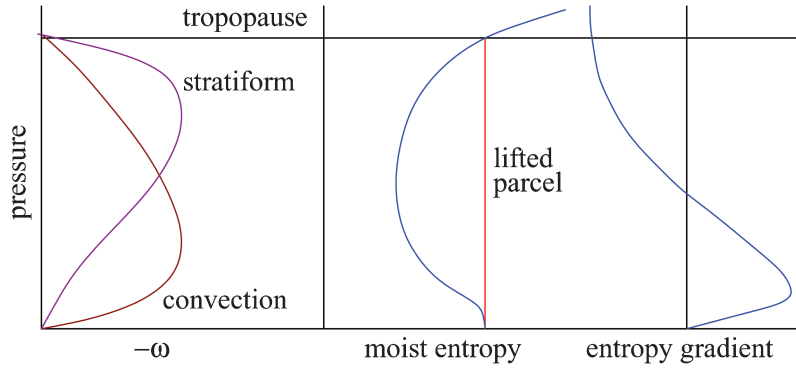
Figure 6. Schematic diagram of a typical tropical profile of moist entropy (middle panel) and its pressure gradient (right panel) with the entropy of a lifted parcel illustrated. Two typical mass flux profiles are illustrated (left panel), a convective profile with a low-level maximum and a stratiform profile with a high-level maximum.

Thus, $\tilde{s}(p)$ in stage 2 may represent an entropy profile quite different from that which would ultimately result in stage 3. The same holds for the mixing ratio on the periphery of the control volume, which is used in the denominator of the NGMS to compute moisture convergence.

Focusing our attention on the vertical advection part of the NGMS (3.3), we note that the crucial element of this calculation is the estimate of $[\bar{\omega}(\partial\tilde{s}/\partial p)]$. Since the moisture divergence is generally negative in convectively active regions, the sign of $\bar{\Gamma}_V$ will follow the sign of $[\bar{\omega}(\partial\tilde{s}/\partial p)]$.

Figure 6 shows a typical profile of moist entropy in the tropics as well as mass flux profiles characteristic of convection and stratiform conditions respectively. The convective profile has a maximum vertical mass flux at low levels while the stratiform mass flux maximum occurs at upper levels in the troposphere (Mapes and Houze 1995). In the convective case $-\bar{\omega}$ is therefore largest at low levels where $\partial\tilde{s}/\partial p > 0$, which means that $[\bar{\omega}(\partial\tilde{s}/\partial p)] < 0$, i. e., the lateral flow imports entropy into the control volume containing the convection, and the NGMS is negative. Conversely, $-\bar{\omega}$ is largest at upper levels in stratiform rain areas where $\partial\tilde{s}/\partial p < 0$, which means that NGMS is positive in this case, and lateral flows export entropy (Sobel 2007). Other things being equal, convective precipitation therefore tends to increase the saturation fraction of the column in which it is embedded, assuming that the temperature profile remains unchanged, while stratiform precipitation tends to decrease the saturation fraction.

4.5. Multiple equilibria

Raymond (2000) showed how the precipitation in a convectively active region would evolve for the case of positive GMS. Figure 7 illustrates the relaxation of precipitation toward a stable equilibrium rate in this case, irrespective of its starting point.

For negative GMS the behavior is more complex. As noted in section 2, López and Raymond (2005) used sounding and airborne Doppler radar observations to document

convective and stratiform mass flux profiles over the west Pacific warm pool and to determine the conditions in which convective and stratiform regimes were respectively dominant. The key parameter turned out to be the saturation deficit, which can be re-expressed as the saturation fraction, assuming a fixed temperature profile. Convective regimes tended to be associated with smaller saturation fractions than stratiform regimes and were demonstrated to import moist entropy, thus exhibiting negative GMS. Stratiform regimes showed the reverse behavior.

Figure 8 shows how the existence of NGMS which changes from negative to positive as the saturation fraction increases modifies the picture of precipitation evolution developed by Raymond (2000). Instead of a single stable solution, one would expect instead an unstable equilibrium solution in the negative NGMS region and a stable solution where NGMS is positive. The resulting evolution of precipitation rate with time is illustrated by three trajectories labeled A, B, and C in figure 8. Trajectory A starts out with precipitation and saturation fraction less than the unstable equilibrium values. The precipitation rate evolves toward zero in this case. Zero precipitation rate thus constitutes a
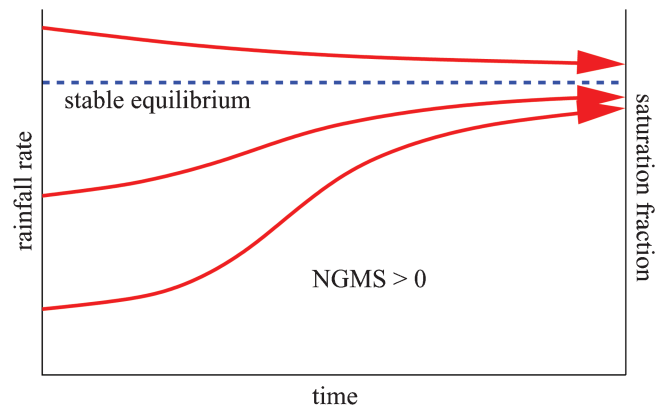

Figure 7. Evolution of the precipitation rate and saturation fraction in an environment where NGMS everywhere positive.
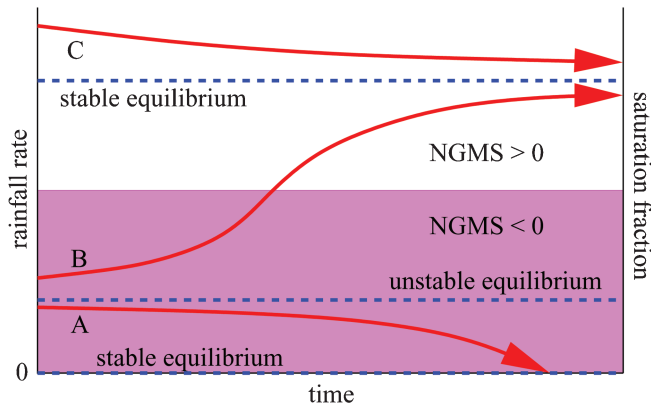
Figure 8. Possible evolution of the precipitation rate and saturation fraction in an environment where NGMS is a function of saturation fraction.

stable equilibrium solution. Trajectories B and C both begin with precipitation rates and saturation fractions in excess of unstable equilibrium values and evolve toward the upper stable equilibrium point. The result is a bistable system, with two stable equilibrium states, a humid, high precipitation state with positive NGMS and a dry, zero precipitation state with negative NGMS, separated by an unstable equilibrium state. Sobel et al. (2007) demonstrated this type of behavior in a single column model of the atmosphere using a cumulus parameterization.

Note that for high precipitation rates where the NGMS is positive, the precipitation itself acts to limit the saturation fraction, since positive NGMS corresponds to the lateral export of moist entropy. Furthermore, for fixed NGMS, heavier precipitation implies more entropy export. Given the steepness of the precipitation rate as a function of saturation fraction, this negative feedback on saturation fraction is likely to be quite "stiff", with little likelihood that saturation fractions above some critical value will occur.

5. The GMS and large-scale flows

The GMS comes into many conceptual models of large-scale flow in the tropics. In this section we discuss a number of such models, showing how the GMS plays different roles in different circumstances.

5.1. Statistical quasi-equilibrium models

Emanuel et al. (1994) presented arguments for the so-called statistical quasi-equilibrium model of interactions between moist convection and the large-scale flow. This model appeared in its original and simplest form in Emanuel's (1987) paper on intraseasonal oscillations. In that paper the temperature profile of the atmosphere is assumed to be that of a moist adiabat with saturated moist entropy equal to that of the moist entropy in the boundary layer. The boundary

layer entropy is determined by budget considerations for entropy over the entire troposphere, since convection is assumed to redistribute entropy vertically in an infinitely short time. Contributors to the entropy budget are surface entropy fluxes, radiative losses, and zonal advection by the mean zonal wind. On an equatorial beta plane with mean surface easterlies, this model produces an unstable, eastward-moving equatorial mode as well as a number of off-equatorial modes. We will focus on the equatorial mode. Both the growth rate and the propagation speed of this mode depend primarily on the horizontal wavenumber and the strength of the mean easterlies. Examination of Emanuel's (1987) governing equations show that his modes reduce to neutral Matsuno (1966) modes with zero equivalent depth (or zero effective stratification) in the absence of mean zonal flow and radiative damping.

Emanuel et al. (1994) expanded the reasoning in Emanuel (1987) in two fundamental ways. First, a lag of order an hour or two between convective forcing and response was introduced. This by itself damps modes. Second, convection was assumed to provide an additional negative tendency on the boundary layer entropy in comparison to Emanuel (1987). Conceptually, this was related to the transport of low entropy air into the boundary layer by convective downdrafts. As demonstrated below, this corresponds to introducing a positive GMS; the original Emanuel (1987) model exhibits zero GMS.

Neelin and Yu (1994) and Yu and Neelin (1994) implemented the ideas of Emanuel et al. (1994) in a linearized equatorial beta plane model using a simplified Betts-Miller (Betts 1986) cumulus parameterization. The thinking behind the Betts-Miller parameterization is very much in accord with the philosophy expressed in Emanuel et al. (1994). Yu and Neelin (1997) expand on these authors' previous work, while Neelin (1997) discusses the role of GMS in tropical circulations. Neelin and Zeng (2000) and Zeng et al. (2000) describe a simplified global circulation model (the quasi-equilibrium tropical circulation model; QTCM) which incorporates the earlier ideas of Neelin and colleagues. This model has been used in numerous studies of the interaction of convection with large-scale flows under varying conditions, e. g., Chou and Neelin (2004), Sobel and Neelin (2006), and Chou et al. (2009). As these authors point out, the GMS plays an important role in analyzing how convection changes with climate change.

In order to expose the fundamental nature of the Neelin-Yu (1994) model, a highly simplified and incomplete version of the original model is presented here. We begin with the two-dimensional, linearized, Boussinesq, non-rotating governing equations for perturbations on an atmosphere at rest, written largely in the notation of Fuchs and Raymond (2007):

$$\frac{\partial u}{\partial t} + \frac{\partial p}{\partial x} = 0 \qquad (5.1)$$

$$\frac{\partial p}{\partial z} - b = 0 \tag{5.2}$$

$$\frac{\partial u}{\partial x} + \frac{\partial w}{\partial z} = 0 \tag{5.3}$$

$$\frac{\partial b}{\partial t} + \Gamma_B w = S_B \tag{5.4}$$

$$\frac{\partial q}{\partial t} + \Gamma_Q w = S_Q \tag{5.5}$$

$$\frac{\partial e}{\partial t} + \Gamma_E w = S_E \tag{5.6}$$

where u and w are the horizontal and vertical velocities, p is the kinematic pressure, b is the buoyancy, equal to the acceleration of gravity times the fractional potential temperature anomaly, and q and e are the mixing ratio and moist entropy perturbations scaled to buoyancy units (Fuchs and Raymond 2007). The quantities Γ_B, Γ_Q, and Γ_E are the ambient vertical gradients of potential temperature, mixing ratio, and moist entropy, also scaled to buoyancy units. Source terms for buoyancy, mixing ratio, and moist entropy are given by S_B, S_Q, and S_E.

The moist entropy equation is redundant (but still useful) since $e = b + q$, $\Gamma_E = \Gamma_B + \Gamma_Q$, and $S_E = S_B + S_Q$. We ignore surface fluxes and radiation in this limited treatment, so that

$$\int_0^h S_E dz = 0 \tag{5.7}$$

where h is the height of the tropopause. The limitation to two-dimensionality eliminates Rossby wave-like modes from the analysis and limits consideration to convectively coupled gravity waves, which have the same zonal structure as equatorial Kelvin waves. As the latter receive most of the attention in Neelin and Yu (1994), this is not a major limitation.

Equations (5.1)-(5.3) can be combined into a single equation relating vertical velocity w and buoyancy b,

$$\frac{\partial^3 w}{\partial t \partial z^2} = \frac{\partial^2 b}{\partial x^2}, \tag{5.8}$$

leaving only the buoyancy to be determined. The simplified Betts-Miller cumulus parameterization consists of the assumptions

$$S_B = -\mu(b - b_0) \tag{5.9}$$

and

$$S_Q = -\mu q \tag{5.10}$$

where μ^{-1} is an adjustment time constant equal to about 2 h. The cumulus parameterization thus has the net effect of relaxing the moisture perturbation toward zero and the buoyancy perturbation toward b_0, which is taken to be independent of height. The parameter b_0 is chosen so that the condition (5.7) on the entropy source term is satisfied. This condition can be expressed

$$\int_0^h (b + q - b_0) dz = \int_0^h (e - b_0) dz = 0. \tag{5.11}$$

Taking the partial derivative of this with respect to time and substituting (5.6) results in

$$\frac{\partial b_0}{\partial t} = -\frac{1}{h} \int_0^h \Gamma_E w dz. \tag{5.12}$$

The GMS can be written in this context as

$$\Gamma_M \equiv \int_0^h \Gamma_E w dz \Big/ \int_0^h \Gamma_B w dz \tag{5.13}$$

(Fuchs and Raymond 2007; Raymond and Fuchs 2009). Eliminating the integral over $\Gamma_E w$ in favor of an integral over $\Gamma_B w$ in (5.12) may be done using this definition:

$$\frac{\partial b_0}{\partial t} = -\frac{\Gamma_M}{h} \int_0^h \Gamma_B w dz. \tag{5.14}$$

Taking the time derivative of the buoyancy equation (5.4) and substituting (5.14) results in

$$\left(\frac{\partial}{\partial t} + \mu\right)\frac{\partial b}{\partial t} = \\ -\Gamma_B \frac{\partial w}{\partial t} - \frac{\mu \Gamma_M}{h} \int_0^h \Gamma_B w dz. \tag{5.15}$$

Elimination of the buoyancy between this equation and (5.8) finally yields

$$\left(\frac{\partial}{\partial t} + \mu\right)\frac{\partial^4 w}{\partial t^2 \partial z^2} + \Gamma_B \frac{\partial^3 w}{\partial t \partial x^2} \\ = -\frac{\mu \Gamma_M}{h} \int_0^h \Gamma_B \frac{\partial^2 w}{\partial x^2} dz. \tag{5.16}$$

This integro-differential equation is difficult to solve analytically. However, Neelin and Yu's assumption for the value of μ makes it much larger in magnitude than the frequency of any plausible large-scale disturbance. If we take the limit of very large μ, then this equation reduces to

$$\frac{\partial^4 w}{\partial t^2 \partial z^2} = -\frac{\Gamma_M}{h} \int_0^h \Gamma_B \frac{\partial^2 w}{\partial x^2} dz \tag{5.17}$$

which is more tractable. In particular, the solution for vertical velocity w takes the form

$$w = W(x,t)z(h - z) \tag{5.18}$$

where we assume that Γ_B is constant and can therefore be extracted from the integral. The parabolic form of this solution in z is not precisely a first baroclinic normal mode, but it is very close to it. The resulting equation is

$$\frac{\partial^2 W}{\partial t^2} - \frac{h^2 \Gamma_M \Gamma_B}{12} \frac{\partial^2 W}{\partial x^2} = 0 \qquad (5.19)$$

which we recognize as the one-dimensional wave equation with constant phase speed c given by

$$c^2 = \frac{h^2 \Gamma_M \Gamma_B}{12}. \qquad (5.20)$$

Since the speed of adiabatic gravity waves with vertical half-wavelength h (i. e., the fundamental baroclinic mode) is $c_a = h\Gamma_B{}^{1/2}/\pi$, this can be written

$$c^2 = \frac{\pi^2 \Gamma_M}{12} c_a^2. \qquad (5.21)$$

If $\Gamma_M \approx 0.1$, we see that $c \approx c_a/3$, or ≈ 16 m s^{-1} for a typical fundamental baroclinic mode gravity wave speed of $c_a = 50$ m s^{-1}.

Thus, in the limit of very large μ, the fundamental convectively coupled mode of the Neelin-Yu system is a neutral, non-dispersive traveling wave. Neelin and Yu (1994) show, in line with the reasoning of Emanuel et al. (1994), that the effect of finite μ is to damp slightly these waves without significantly affecting their phase speed. Furthermore, these waves can be destabilized if wave-induced surface heat exchange (WISHE; Yano and Emanuel 1991) becomes active in an environment with non-zero mean zonal surface flow. This solution reduces to the (trivial) case of no WISHE in Emanuel (1987) when $\Gamma_M = 0$.

Modes with vertical structure different than that given by (5.18) are not admitted as solutions to (5.17). Neelin and Yu (1994) show that such solutions exist in the case of non-zero μ, but are very strongly damped.

The most interesting result is that the square of the convectively coupled gravity wave propagation speed (or the equivalent depth) is proportional to the GMS. Furthermore, according to Emanuel et al. (1994), positive GMS arises from the existence of convective downdrafts which carry low moist entropy air from the free troposphere into the boundary layer. This is in accord with the picture of GMS presented in figure 6, since downdraft mass fluxes reduce the updraft mass flux at low to middle levels, thus causing the maximum vertical mass flux to occur at higher levels.

Neelin and Yu (1994) and Yu and Neelin (1994) also found stationary deep convective modes. These are modes which don't propagate except by advection and whose essential dynamics consists just of the interaction of convection and moisture in a single column. They satisfy the condition expressed in Neelin and Yu's equation (5.9h), which can be expressed in our terms as

$$\int_d^h \Gamma_E w dz + \int_0^d \Gamma_E w dz = \int_0^h \Gamma_E w dz = 0 \qquad (5.22)$$

where d is the boundary layer thickness. The second term on the left side of this equation is equivalent to their boundary layer term, given their bulk boundary layer model. Comparison with (5.13) indicates that (5.22) is equivalent to $\Gamma_M = 0$. In our simplified representation these modes thus correspond to their convectively coupled modes with zero GMS. However, given that Neelin and Yu (1994) assume an additional degree of freedom in the form of an explicit boundary layer, these modes appear to have an independent existence in their model.

Though not considered by Neelin and Yu (1994), their mathematical model admits solutions with negative GMS. Making $\Gamma_M < 0$ in (5.19) results in pairs of stationary modes which respectively amplify and decay with time. However, in the context of Emanuel et al. (1994), negative GMS doesn't make physical sense, since it requires convective downdrafts to increase rather than decrease the moist entropy (or moist static energy) of the atmospheric boundary layer. Below we consider an extension to their model in which negative GMS occurs in a physically plausible manner.

5.2. Negative GMS and the ITCZ

Back and Bretherton (2006) showed, using reanalysis data, that the east Pacific intertropical convergence zone (ITCZ) exhibits negative Γ_V (vertical advection) and positive Γ_H (horizontal advection) with an indeterminate sum Γ_R. Thus, ITCZ convection has negative GMS in the classical sense of Neelin and Held (1987) and Yu et al. (1998), but the resulting source of moist static energy is removed by horizontal advection. As noted above, this is a situation not envisioned by Neelin and Yu (1994), where the target relative humidity is held constant with height. However, since Neelin's Quasi-equilibrium Tropical Circulation Model (QTCM; Neelin and Zeng 2000; Zeng et al. 2000) has more freedom in the choice of target relative humidity profile, negative GMS values can in principle occur there.

Sobel and Neelin (2006) developed a hybrid model which includes an explicit prognostic boundary layer of fixed depth coupled to a free troposphere model similar to that in the original QTCM. The convergence occurring in the boundary layer produces divergence distributed uniformly through the depth of the free troposphere with the associated upward motion profile supplementing that produced by normal QTCM mechanisms. The advection of potential temperature and moisture associated with this upward motion enhances convection produced by the QTCM vertical velocity profile. Due to the "bottom-heavy" structure of this boundary layer-driven ascent, the resulting GMS is highly negative. However, the GMS associated with the normal free tropospheric vertical velocity profile is positive. The net GMS is an average of the two weighted by the relative amplitudes of

the two modes of ascent. This hybrid model is thus a way to incorporate the observed behavior of ITCZs into the QTCM.

Crudely, one can think of the boundary layer mode as representing the shallow meridional circulation described by Zhang et al. (2004). This mode imports entropy where there is surface convergence, which can occur in the absence of deep convection when the horizontal variations in sea surface temperature favor it by the Lindzen-Nigam (1987) mechanism. Sobel and Neelin (2006) argued that since the shallow Lindzen-Nigam flow can exist independently of the presence or absence of deep convection, the entropy (or in their case, moist static energy) imported by that flow can be considered as an external forcing on the local entropy budget, similar to the entropy forcing $F_s - R$ in (2.1). In the absence of other processes, the presence and intensity of the deep baroclinic flow, which is strongly coupled to deep convection, then balances that import plus $F_s - R$ through its own gross moist stability. Such an argument is not completely clean because the surface convergence and shallow entropy import are modulated by the pressure gradients due to the deep baroclinic flow so that the two are not truly independent. Nonetheless the recent analysis of Back and Bretherton (2009a,b) also seems to support this view.

In the Sobel and Neelin (2006) model, which is zonally symmetric, a horizontal diffusion of moisture (and thus entropy or moist static energy) had to be introduced in order to reduce the ITCZ intensity to observed levels. This was done out of expediency, but it was then argued that perhaps the diffusion might be standing in for transient non-axisymmetric disturbances, such as easterly waves, which might be exporting moisture from the ITCZ to drier adjacent regions. In the model, the dominant balance in the moist static energy budget is between export by this diffusion and net import by the resolved, zonally symmetric flow (including the strong import by the boundary layer mode and much weaker export by the baroclinic mode). The recent diagnostic work of Peters et al. (2008) supports this picture, with the moist static energy transport by transients out of the east Pacific ITCZ being both significant and diffusive in character. The resulting picture is very different from the early Neelin-Held concept of deep convective regions. In that picture, the net entropy forcing by surface fluxes minus radiative cooling was balanced by export due to the mean divergent circulation, with a positive gross moist stability. In the revised picture of Sobel and Neelin (2006) transient eddy fluxes play an important role in balancing the net source (at least for the east Pacific ITCZ), while the mean circulation may either weakly export or even import entropy, adding to rather than balancing the net source.

5.3. Moisture and Kelvin modes

The statistical quasi-equilibrium models discussed above have the characteristic that vertical structure inconsistent with their assumed first baroclinic mode structure is rapidly damped. Thus, disturbances for which such alternative vertical structure is an intrinsic characteristic cannot be represented by such models. Examples of disturbances of this type include easterly waves (Reed and Recker 1971; Reed et al. 1977; Cho and Jenkins 1987), convectively coupled equatorial Kelvin waves (Straub and Kiladis 2002; Tulich et al. 2007), and possibly the Madden-Julian oscillation (Kiladis et al. 2005). Thus, Emanuel et al.'s (1994) elegant idea for determining the vertical structure of tropical disturbances may be over-simplified.

An alternative class of convectively coupled wave models was originated by Mapes (2000) and expanded upon by Majda and Shefter (2001a,b), Majda et al. (2004), Khouider and Majda (2006, 2007, 2008), Kuang (2008a,b), Andersen and Kuang (2008), etc. In such models convection is controlled by convective inhibition, or alternatively convective available potential energy concentrated in the lower troposphere, which essentially amounts to the same thing. These models produce unstable waves which exhibit vertical structure incorporating both first and second baroclinic modes. They typically predict wave speeds in reasonable agreement with the observed propagation speeds of equatorial, convectively coupled Kelvin waves.

A different type of mode was predicted by the simplified models of Sobel et al. (2001) and Fuchs and Raymond (2002, 2005). In these models the precipitation is controlled by the saturation fraction of the troposphere, as described in section 4.2. In the case of no surface mean wind or cloud-radiation interactions, stationary unstable modes with relatively little scale selection develop when the GMS is negative. If surface easterlies are imposed, WISHE causes eastward propagation, with longer wavelength modes propagating more rapidly. With meridional moisture gradients, these modes become unstable for weakly positive GMS. Cloud-radiation interactions can destabilize these modes in the presence of weakly positive GMS as well. The modes predicted by these models were denoted "moisture waves" by Sobel et al. (2001) and "moisture modes" by Fuchs and Raymond (2005), since moisture anomalies play an important dynamical role in their development.

As noted previously, Neelin and Yu (1994) and Yu and Neelin (1994) discovered similar modes in the context of their quasi-equilibrium model, which they called "kinematically dominated modes" or "stationary deep convective modes" (see the discussion in section 5.1), though their focus at the time was on the propagating convective modes predicted by their model. Moisture modes also arise in the mesoscale simulations with parameterized convection by Sobel and Bretherton (2003) as well as in the three-dimensional, cloud-resolving simulations of Tompkins (2001), Bretherton et al. (2005), and Stephens et al. (2008).

The simplicity of the moisture mode allows its essence to be captured in weak temperature gradient cloud resolving model simulations such as those of Raymond and Zeng (2005) and Raymond and Sessions (2007). This is because the interaction between neighboring air columns is via the

rapid buoyancy equilibration and the exchange of moisture between columns implied by the weak temperature gradient approximation. In fact, it is fair to say that the moisture mode is what remains after the weak temperature gradient approximation is made, just as only balanced modes survive the quasi-geostrophic approximation (Sobel et al. 2001).

Fuchs and Raymond (2002, 2005) assumed a first baroclinic mode vertical structure for both the heating and the vertical velocity structure of moisture modes. Fuchs and Raymond (2007) relaxed this condition, keeping the sinusoidal heating with a half-wavelength equal to the depth of the tropopause, but implementing a vertically resolved dynamical model including an upper radiation boundary condition. The results are similar to those of Fuchs and Raymond (2002) for moisture modes, though they differ greatly for convectively coupled gravity modes.

Raymond and Fuchs (2007) extended the model of Fuchs and Raymond (2007) by including an additional control on convection from convective inhibition, which we describe here. Starting from (5.1)-(5.4) and assuming time and zonal dependencies of the form $\exp[i(kx - \omega t)]$ yields

$$\frac{d^2 w(z)}{dz^2} + m^2 w(z) = \frac{k^2}{\omega^2} S_B(z), \qquad (5.23)$$

$$b = (i/\omega)(S_B - \Gamma_B w), \qquad (5.24)$$

$$e = (i/\omega)(S_E - \Gamma_E w), \qquad (5.25)$$

where $m = k\Gamma_B^{1/2}/\omega$. The convective heating takes the first baroclinic mode form

$$S_B(z) = (m_0 B/2)\sin(m_0 z) \qquad (5.26)$$

where $m_0 = \pi/h$, h being the height of the tropopause, and B is a constant determined below by the convective closure.

As with our simplified discussion of the Neelin-Yu (1994) model, cloud-radiation interactions and WISHE are ignored. The convective closure condition is

$$\int_0^h S_B dz = B$$
$$= \alpha \int_0^h q(z)dz + \mu_{CIN}(e_s - e_t) \qquad (5.27)$$

where α^{-1} is a time constant of order one day and $q(z)$ is the vertical profile of scaled mixing ratio perturbation as before. The first term on the right side of (5.27) represents the effects of perturbations in precipitable water and is responsible for producing moisture modes, whereas the second term results in convectively coupled gravity waves, with the constant μ_{CIN} governing the strength of the convective inhibition effect. In this term e_s is the scaled surface moist entropy perturbation and is set to zero in the absence of WISHE. The quantity e_t is the perturbation saturation moist entropy at the top of the planetary boundary layer (PBL), the height of which is indicated by the dimensionless parameter D, the ratio of PBL to tropopause height h. Since e_t is a function only of the buoyancy perturbation b and pressure, $e_t = \lambda_t b(D)$, where $b(D)$ is b at the PBL top, with $\lambda_t \approx 3.5$.

Using $q(z) = e(z) - b(z)$ as well as (5.7), (5.13), (5.24), and (5.25) allows (5.27) to be rewritten as

$$B = \frac{1 - \Gamma_M}{1 - i\kappa\Phi}\int_0^h \Gamma_B w dz + \frac{i\kappa\mu_{CIN}\lambda_t \Phi b(D)}{1 - i\kappa\Phi} \qquad (5.28)$$

where Γ_M is the GMS as defined by (5.13), $\kappa = h\Gamma_B^{1/2}k/(\pi a)$ is the dimensionless wavenumber, and where $\Phi = m_0/m = \pi\omega/(kh\Gamma_B^{1/2})$ is the phase speed ω/k of the disturbance divided by $h\Gamma_B^{1/2}/\pi$, the phase speed of free, fundamental baroclinic mode gravity waves.

The solution to (5.23)-(5.24) in terms of B is

$$w(z) =$$
$$\frac{m_0 B\left[\sin(m_0 z) + \Phi e^{-i\pi/\Phi}\sin(m_0 z/\Phi)\right]}{2\Gamma_B(1 - \Phi^2)} \qquad (5.29)$$

and

$$b(z) =$$
$$-\frac{i m_0 B\left[\Phi \sin(m_0 z) + e^{-i\pi/\Phi}\sin(m_0 z/\Phi)\right]}{2\alpha\kappa(1 - \Phi^2)}. \qquad (5.30)$$

The first term on the right side of (5.29) is the inhomogeneous part of the solution to (5.23), whereas the second term is the homogeneous part. Since physically the homogeneous solution represents a free gravity wave in the troposphere with dimensionless phase speed Φ, it is this part of the solution which sets the phase speed of the disturbance. It also has a vertical structure significantly different from that of the fundamental baroclinic mode.

Combination of (5.28), (5.29), and (5.30) results in a rather complex dispersion relation for Φ,

$$\kappa\Phi^3 + i\Phi^2 - \kappa\Phi - i + i(1 - \Gamma_M)F(\Phi)$$
$$+ \frac{i\Phi\mu_{CIN}\lambda_t m_0}{2\alpha}L(D,\Phi) = 0, \qquad (5.31)$$

where

$$F(\Phi) = 1 + \frac{\Phi^2}{2}e^{-i\pi/\Phi}\left[1 - \cos\left(\frac{\pi}{\Phi}\right)\right] \qquad (5.32)$$

and

$$L(D,\Phi) = e^{-i\pi/\Phi}\sin\left(\frac{\pi D}{\Phi}\right) + \Phi\sin(\pi D), \qquad (5.33)$$

which can only be solved numerically. However, if we ignore convective inhibition by setting $\mu_{CIN} = 0$ and keep leading

order terms in $|\Phi| \ll 1$, it is easily shown that the dispersion relation reduces to

$$\Phi \approx -i\Gamma_M/\kappa, \qquad (5.34)$$

i. e., the mode is stationary with a growth rate proportional to minus the GMS. Thus, negative GMS results in moisture mode instability as one might expect.

If on the other hand, we suppress moisture modes by setting $\Gamma_M = 0$ and again retain only leading order terms in $|\Phi|$, then the simplified, but still implicit dispersion relation

$$i\kappa + \frac{m_0\lambda_t\mu_{CIN}}{2\alpha}e^{-i\pi/\Phi}\sin\left(\frac{m_0 D}{\Phi}\right) = 0 \qquad (5.35)$$

holds. If Φ is approximately real, reflecting propagation with a modest growth rate, then the exponential term must be negative imaginary, implying that

$$|\Phi| \approx \frac{2}{1+4n} \qquad (5.36)$$

where n is a positive integer. (The value $n = 0$ formally satisfies (5.35), but violates the condition that $|\Phi| \ll 1$.) For $n = 1$ the phase speed is 20 m s^{-1} if the free, fundamental mode gravity wave speed is 50 m s^{-1}. This is quite close to the observed propagation speed of convectively coupled equatorial Kelvin waves. Furthermore, unlike the Neelin-Yu (1994) and similar statistical quasi-equilibrium solutions, it depends only weakly on the GMS (see Raymond and Fuchs 2009) and it exhibits a vertical structure similar to that seen in observed Kelvin waves.

The complex vertical structure of temperature and wind in this model is produced by a fundamental baroclinic mode heating profile, in contrast to the results of Mapes (2000) etc. This is not to say that the pattern of convective heating assumed by these authors does not exist in real Kelvin waves – only that it is not strictly necessary to produce the observed structure of the waves.

When the full dispersion relation is analyzed numerically, both moisture modes and convectively coupled gravity waves emerge, with only modest modifications to the results discussed above.

5.4. GMS and the MJO

There are many theories for the Madden-Julian oscillation (MJO; see Zhang 2005 for a comprehensive review). Nevertheless, most global atmospheric numerical models have failed to provide a realistic representation of this phenomenon (Slingo 1996; Lin 2006).

Raymond and Fuchs (2009) demonstrated robust MJO-like disturbances in an equatorial beta plane model with no land, but with realistic sea surface temperatures and a toy convective parameterization prone to the production of negative GMS in strong convection. Figure 9 shows a snapshot of precipitation, surface wind, saturation fraction, and NGMS in an active MJO phase in the eastern Indian

Ocean and western Pacific for a perpetual August simulation. Notice how the convection organizes itself into a line with a long near-equatorial component somewhat like a monsoon trough or an ITCZ. Meridional oscillations in the line suggest the development of largescale dynamical instability. Further examination shows that some of the oscillations break off to form vortices which resemble the outer circulations of a tropical cyclone.

An interesting feature of this simulation is that the existence of strong convection within these lines coincides with the development of negative NGMS. This invites comparison with the results discussed in section 5.2 of Back and Bretherton (2006) and Sobel and Neelin (2006), who infer the existence of negative GMS in the east Pacific ITCZ and suggest that it is a consequence of the boundary layer flow produced by strong sea surface temperature gradients in this region. However, the negative GMS in the simulation shown in figure 9 occurs in convective lines over weak sea surface temperature gradients where boundary layer forcing produced by these gradients is unlikely to be as important as it is in the east Pacific.

As figure 10 shows, for precipitation rates between 5 mm d^{-1} and 10 mm d^{-1} the convective mass flux profile is characteristic of cumulus congestus clouds with a maximum in vertical mass flux near 800 hPa, which is well below the level of minimum moist entropy, resulting in negative
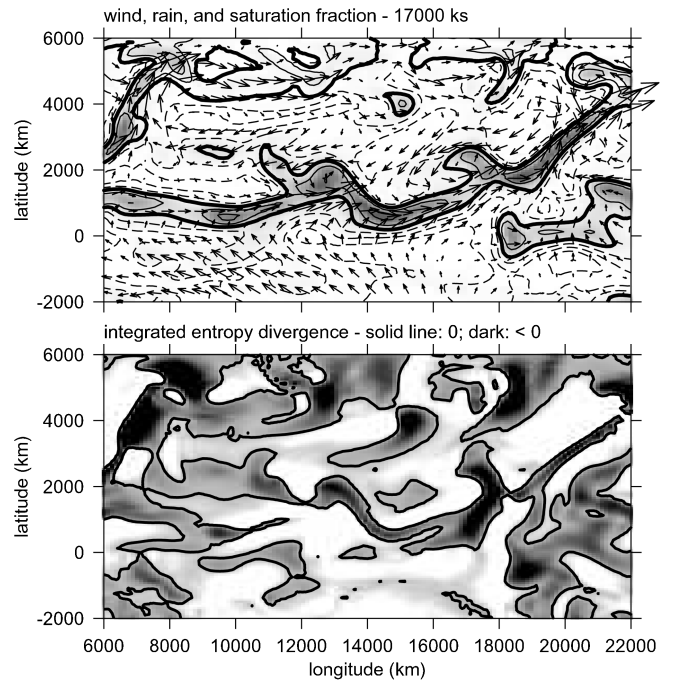

Figure 9. Snapshot of convection in the eastern Indian Ocean and western Pacific during an active MJO phase in the beta plane numerical model of Raymond and Fuchs (2009). (a) Surface wind, precipitation rate (shading) and saturation fraction (contours). (b) NGMS, with the heavy line indicating a zero value, light shading positive values, and dark shading negative values.
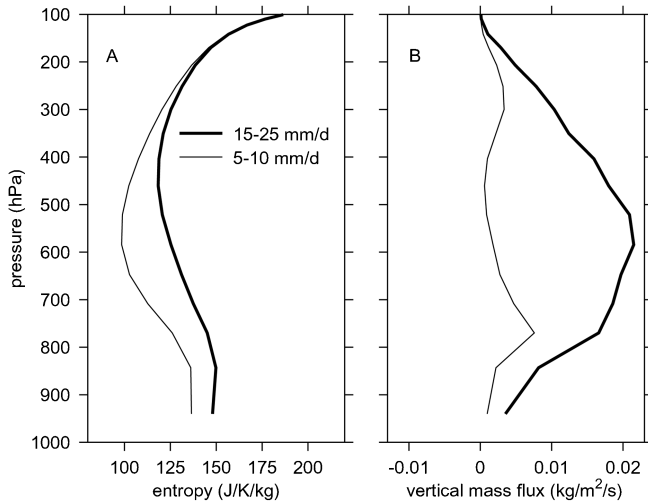
Figure 10. Vertical profiles of (a) specific moist entropy and (b) vertical mass flux, averaged over regions in figure 9 with precipitation rates in the ranges 5 – 10 mm d^{-1} (thin lines) and 15 – 25 mm d^{-1} (thick lines).

GMS (see figure 6). However for stronger precipitation, figure 10 shows that the level of maximum vertical mass flux ascends to near 550 hPa. Negative GMS results from the development in this case of a moist entropy profile with a minimum at even higher levels.

Whether the manner in which this model produces negative GMS actually occurs in nature remains to be determined. However, the existence of negative GMS, however produced, strongly suggests that the moisture mode instability discussed in section 5.3 is active in this model. This conclusion is supported by the strong correlation between precipitation and saturation fraction illustrated in figure 9 as well as the tendency of the disturbances to move rather slowly. In this model at least, the MJO appears to be a moisture mode which depends on the transient occurrence of negative GMS for its existence.

6. Summary and conclusions

In developing a consistent framework for the idea of gross moist stability, we draw on a great deal of previous work by ourselves and others. The first problem addressed is to how to define gross moist stability – many different definitions exist in the literature. We choose to adopt the normalized gross moist stability (NGMS) of Raymond and Sessions (2007) and Raymond et al. (2007). This differs from the classic gross moist stability proposed by Neelin and Held (1987) and extended by Yu et al. (1998) in that it (1) normalizes with the moisture convergence rather than the mass convergence; (2) includes the horizontal advection or ventilation term neglected in the above work; and (3) uses the specific moist entropy rather than the moist static energy as the quasi-conserved thermodynamic variable. Unlike the classic gross moist stability, the NGMS is dimensionless.

As the numerator and denominator of the NGMS are both expressed as horizontal divergences, the logical way to obtain the NGMS averaged over a region is to average horizontally the numerator and denominator separately and define the average NGMS as the ratio of these quantities.

The NGMS becomes an important component in a predictive theory for precipitation if the precipitation rate can be expressed as a function of something related to the vertically integrated moist entropy in the tropospheric column. This is because the numerator of the NGMS is the horizontal entropy divergence, which is the most uncertain quantity in the moist entropy budget equation, while the denominator is the net moisture convergence, which is closely related to the precipitation rate. The key parameter related to the specific moist entropy s is the saturation fraction, which can be expressed to reasonable accuracy as

$$S = \frac{[s - s_d]}{[s_s - s_d]} \quad (6.1)$$

where s_s is the saturated moist entropy, s_d is the specific dry entropy, and where the square brackets indicate a pressure integral over the full troposphere. The precipitation rate, at least over warm tropical oceans, turns out to be a highly inelastic function of saturation fraction, with nearly zero rain for $S < 0.7$, and asymptoting to large precipitation rates for $S \approx 0.87$ in our work. This steeply increasing precipitation rate as a function of saturation fraction is one key to developing sufficiently vigorous synoptic and intraseasonal convective modes in the large-scale numerical model of Raymond (2007).

Given the role of NGMS in ''summarizing our ignorance about convection'', it is noteworthy that the boundary layer quasi-equilibrium theory of Raymond (1995) and Emanuel (1995) provides one possible route to understanding how the NGMS is determined. Convection is controlled in this theory via a balance between the tendency of surface fluxes of heat and moisture to increase boundary layer moist entropy and the countervailing tendency of convective downdrafts to decrease it. The downdraft moist entropy flux into the boundary layer is related by cloud physics and dynamics to the updraft mass flux, with drier, more unstable environments leading to a stronger downdraft flux per unit updraft. The precipitation rate is likewise related to environmental conditions, with a moister troposphere yielding more rain. A simple theoretical model of the GMS invoking boundary layer quasi-equilibrium is introduced here for the purpose of increasing understanding, but numerical cloud modeling using the weak temperature gradient approximation provides a more quantitative route to the determination of NGMS as a function of environmental conditions.

It is important to understand the difference between the NGMS in statistically steady conditions and in unsteady conditions. In the steady case the NGMS is constrained by the relationship between the entropy forcing and the

precipitation rate. In this situation the NGMS cannot be negative, except in the case of zero precipitation, as any steady state with negative NGMS and nonzero rain will be unstable. However, this constraint does not exist in unsteady conditions. In the unsteady case the sign of the NGMS is a function of the vertical convective/mesoscale mass flux profile, at least in the case in which horizontal advection and ventilation are negligible. Negative NGMS arises from purely convective, or bottom-heavy vertical mass flux profiles, whereas positive NGMS is associated with top-heavy stratiform mass flux profiles.

López and Raymond (2005) showed that stratiform profiles were favored by very moist environments, i. e., those with high saturation fraction. On the other hand, drier environments favored convective profiles. We demonstrated that this situation is likely to lead to multiple equilibria, with a given surface wind speed being associated with either no precipitation and a very dry troposphere or ample precipitation and a very moist troposphere. This behavior may be responsible for the observed bistable humidity structure of the tropical troposphere (Zhang et al. 2003).

The GMS plays an important role in large-scale dynamics in the tropics. In the Emanuel et al. (1994) statistical quasi-equilibrium theory the GMS is always taken to be positive and tropical wave disturbances propagate at speeds which scale with the square root of the GMS. However, in the model of Raymond and Fuchs (2007), rapidly moving convectively coupled waves such as the equatorial Kelvin wave are relatively insensitive to the GMS, while the more slowly moving moisture modes only occur when the GMS is negative, or at least when the auxiliary effects of cloud-radiation interactions (Fuchs and Raymond 2002) or surface flux anomalies correlated with convection (Sugiyama 2009) act to create an "effective" negative GMS even when the GMS itself is positive. Negative GMS may play important roles in the dynamics of ITCZs and the MJO.

We have demonstrated that the concept of gross moist stability leads to a number of fruitful lines of inquiry in the interaction of moist convection with the tropical environment. We expect that this work will lead ultimately to a deeper understanding of this important area of atmospheric dynamics.

References

Andersen, J. A. and Z. Kuang, 2008: A toy model of the instability in the equatorially trapped convectively coupled waves on the equatorial beta plane. *J. Atmos. Sci.*, **65**, 3736–3757, doi: 10.1175/2008JAS2776.1.

Back, L. E., and C. S. Bretherton, 2005: The relationship between wind speed and precipitation in the Pacific ITCZ. *J. Climate*, **18**, 4317–4328, doi: 10.1175/JCLI3519.1.

Back, L., E., and C. S. Bretherton, 2006: Geographic variability in the export of moist static energy and vertical motion profiles in the tropical Pacific. *Geophys. Res. Letters*, **33**, L17810, doi: 10.1029/2006GL026672.

Back, L. E., and C. S. Bretherton, 2009a: On the relationship between SST gradients, boundary layer winds and convergence over tropical oceans. *J. Climate*, **22**, 4182–4196, doi: 10.1175/2009JCLI2392.1.

Back, L. E., and C. S. Bretherton, 2009b: A simple model of climatological rainfall and vertical motion patterns over the tropical oceans. *J. Climate*, in press, doi: 10.1175/2009JCLI2393.1.

Betts, A. K., 1974: Further comments on "A comparison of the equivalent potential temperature and the static energy". *J. Atmos. Sci.*, **31**, 1713–1715, doi: 10.1175/1520-0469(1974)031<1713:FCOCOT>2.0.CO;2.

Betts, A. K., 1986: A new convective adjustment scheme. Part I: Observational and theoretical basis. *Quart. J. Roy. Meteor. Soc.*, **112**, 677–691, doi: 10.1002/qj.49711247307.

Bretherton, C. S., and P. K. Smolarkiewicz, 1989: Gravity waves, compensating subsidence and detrainment around cumulus clouds. *J. Atmos. Sci.*, **46**, 740–759, doi: 10.1175/1520-0469(1989)046<0740:GWCSAD>2.0.CO;2.

Bretherton, C. S., M. E. Peters, and L. E. Back, 2004: Relationships between water vapor path and precipitation over the tropical oceans. *J. Climate*, **17**, 1517–1528, doi: 10.1175/1520-0442(2004)017<1517:RBWVPA>2.0.CO;2.

Bretherton, C. S., P. N. Blossey, and M. Khairoutdinov, 2005: An energy-balance analysis of deep convective self-aggregation above uniform SST. *J. Atmos. Sci.*, **62**, 4273–4292, doi: 10.1175/JAS3614.1.

Cho, H.-R., and M. A. Jenkins, 1987: The thermal structure of tropical easterly waves. *J. Atmos. Sci.*, **44**, 2531–2539, doi: 10.1175/1520-0469(1987)044<2531:TTSOTE>2.0.CO;2.

Chou, C., and J. D. Neelin, 2004: Mechanisms of global warming impacts on regional tropical precipitation. *J. Climate*, **17**, 2688–2701, doi: 10.1175/1520-0442(2004)017<2688:MOGWIO>2.0.CO;2.

Chou, C., J. D. Neelin, C.-A. Chen, and J.-Y. Yu, 2009: Evaluating the "rich-get-richer" mechanism in tropical precipitation change under global warming. *J. Climate*, **22**, 1982–2005, doi: 10.1175/2008JCLI2471.1.

Derbyshire, S. H., I. Beau, P. Bechtold, J.-Y. Grandpeix, J.-M. Piriou, J.-L. Redelsperger, and P. M. M. Soares, 2004: Sensitivity of moist convection to environmental humidity. *Quart. J. Roy. Meteor. Soc.*, **130**, 3055–3079, doi: 10.1256/qj.03.130.

Emanuel, K. A., 1987: An air-sea interaction model of intraseasonal oscillations in the tropics. *J. Atmos. Sci.*,

44, 2324–2340, doi: 10.1175/1520-0469(1987)044<2324:AASIMO>2.0.CO;2.

Emanuel, K. A., 1995: The behavior of a simple hurricane model using a convective scheme based on subcloud-layer entropy equilibrium. *J. Atmos. Sci.*, **52**, 3960–3968, doi: 10.1175/1520-0469(1995)052<3960:TBOASH>2.0.CO;2.

Emanuel, K. A., J. D. Neelin, and C. S. Bretherton, 1994: On large-scale circulations in convecting atmospheres. *Quart. J. Roy. Meteor. Soc.*, **120**, 1111–1143, doi: 10.1002/qj.49712051902.

Fuchs, Ž., and D. J. Raymond, 2002: Large-scale modes of a nonrotating atmosphere with water vapor and cloud-radiation feedbacks. *J. Atmos. Sci.*, **59**, 1669–1679, doi: 10.1175/1520-0469(2002)059<1669:LSMOAN>2.0.CO;2.

Fuchs, Ž., and D. J. Raymond, 2005: Large-scale modes in a rotating atmosphere with radiative-convective instability and WISHE. *J. Atmos. Sci.*, **62**, 4084–4094, doi: 10.1175/JAS3582.1.

Fuchs, Ž. and D. J. Raymond, 2007: A simple, vertically resolved model of tropical disturbances with a humidity closure. *Tellus*, **59**A, 344–354, doi: 10.1111/j.1600-0870.2007.00230.x.

Khouider, B., and A. J. Majda, 2006: A simple multicloud parameterization for convectively coupled tropical waves. Part I: Linear analysis. *J. Atmos. Sci.*, **63**, 1308–1323, doi: 10.1175/JAS3677.1.

Khouider, B., and A. J. Majda, 2007: A simple multicloud parameterization for convectively coupled tropical waves. Part II: Nonlinear simulations. *J. Atmos. Sci.*, **64**, 381–400, doi: 10.1175/JAS3833.1.

Khouider, B., and A. J. Majda, 2008: Multicloud models for organized tropical convection: Enhanced congestus heating. *J. Atmos. Sci.*, **65**, 895–914, doi: 10.1175/2007JAS2408.1.

Kiladis, G. N., K. H. Straub, and P. T. Haertel, 2005: Zonal and vertical structure of the Madden-Julian oscillation. *J. Atmos. Sci.*, **62**, 2790–2809, doi: 10.1175/JAS3520.1.

Kuang, Z., 2008a: Modeling the interaction between cumulus convection and linear gravity waves using a limited-domain cloud system-resolving model. *J. Atmos. Sci.*, **65**, 576–591, doi: 10.1175/2007JAS2399.1.

Kuang, Z., 2008b: A moisture-stratiform instability for convectively coupled waves. *J. Atmos. Sci.*, **65**, 834–854, doi: 10.1175/2007JAS2444.1.

Lin, J. L., G. N. Kiladis, B. E. Mapes, K. M. Weickmann, K. R. Sperber, W. Lin, M. C. Wheeler, S. D. Schubert, A. Del Genio, L. J. Donner, S. Emori, J.-F. Gueremy, F. Hourdin, P. J. Rasch, E. Roeckner, and J. F. Scinocca, 2006: Tropical intraseasonal variability in 14 IPCC AR4 climate models part I: Convective signals. *J. Climate*, **19**, 2665–2690, doi: 10.1175/JCLI3735.1.

Lindzen, R. S., and S. Nigam, 1987: On the role of sea surface temperature gradients in forcing low-level winds and convergence in the tropics. *J. Atmos. Sci.*,

44, 2418–2436, doi: 10.1175/1520-0469(1987)044<2418:OTROSS>2.0.CO;2.

López Carrillo, C., and D. J. Raymond, 2005: Moisture tendency equations in a tropical atmosphere. *J. Atmos. Sci.*, **62**, 1601–1613, doi: 10.1175/JAS3424.1.

Lucas, C., E. J. Zipser, and B. S. Ferrier, 2000: Sensitivity of tropical west Pacific oceanic squall lines to tropospheric wind and moisture profiles. *J. Atmos. Sci.*, **57**, 2351–2373, doi: 10.1175/1520-0469(2000)057<2351:SOTWPO>2.0.CO;2.

Madden, R. A., and F. E. Robitaille, 1970: A comparison of the equivalent potential temperature and the static energy. *J. Atmos. Sci.*, **27**, 327–329, doi: 10.1175/1520-0469(1970)027<0327:ACOTEP>2.0.CO;2.

Majda, A. J., and M. G. Shefter, 2001a: Waves and instabilities for model tropical convective parameterizations. *J. Atmos. Sci.*, **58**, 896–914, doi: 10.1175/1520-0469(2001)058<0896:WAIFMT>2.0.CO;2.

Majda, A. J., and M. G. Shefter, 2001b: Models for stratiform instability and convectively coupled waves. *J. Atmos. Sci.*, **58**, 1567–1584, doi: 10.1175/1520-0469(2001)058<1567:MFSIAC>2.0.CO;2.

Majda, A. J., B. Khouider, G. N. Kiladis, K. H. Straub, and M. G. Shefter, 2004: A model for convectively coupled tropical waves: Nonlinearity, rotation, and comparison with observations. *J. Atmos. Sci.*, **61**, 2188–2205, doi: 10.1175/1520-0469(2004)061<2188:AMFCCT>2.0.CO;2.

Mapes, B. E., 2000: Convective inhibition, subgrid-scale triggering energy, and stratiform instability in a toy tropical wave model. *J. Atmos. Sci.*, **57**, 1515–1535, doi: 10.1175/1520-0469(2000)057<1515:CISSTE>2.0.CO;2.

Mapes, B., and R. A. Houze, Jr., 1995: Diabatic divergence profiles in western Pacific mesoscale convective systems. *J. Atmos. Sci.*, **52**, 1807–1828, doi: 10.1175/1520-0469(1995)052<1807:DDPIWP>2.0.CO;2.

Marín, J. C., D. J. Raymond, and G. B. Raga, 2009: Intensification of tropical cyclones in the GFS model. *Atmos. Chem. Phys.*, **9**, 1407–1417.

Matsuno, T., 1966: Quasi-geostrophic motions in the equatorial area. *J. Meteor. Soc. Japan*, **44**, 25–43.

Neelin, J. D., and J.-Y. Yu, 1994: Modes of tropical variability under convective adjustment and the Madden-Julian oscillation. Part I: Analytical theory. *J. Atmos. Sci.*, **51**, 1876–1894, doi: 10.1175/1520-0469(1994)051<1876:MOTVUC>2.0.CO;2.

Neelin, J. D., 1997: Implications of convective quasiequilibrium for the large-scale flow. *The Physics and Parameterization of Moist Atmospheric Convection, Ed. R. K. Smith*, Kluwer, 413–446.

Neelin, J. D., and N. Zeng, 2000: A quasi-equilibrium tropical circulation model – formulation. *J. Atmos. Sci.*, **57**, 1741–1766, doi: 10.1175/1520-0469(2000)057<1741:AQETCM>2.0.CO;2.

Pauluis, O., and I. M. Held, 2002a: Entropy budget of an atmosphere in radiative-convective equilibrium. Part I:

Maximum work and frictional dissipation. *J. Atmos. Sci.*, **59**, 125–139, doi: 10.1175/1520-0469(2002)059<0125:EBOAAI>2.0.CO;2.

Pauluis, O., and I. M. Held, 2002b: Entropy budget of an atmosphere in radiative-convective equilibrium. Part II: Latent heat transport and moist processes. *J. Atmos. Sci.*, **59**, 140–149, doi: 10.1175/1520-0469(2002)059<0140:EBOAAI>2.0.CO;2.

Peters, M. E., Z. Kuang, and C. C. Walker, 2008: Analysis of atmospheric energy transport in ERA-40 and implications for simple models of the mean tropical circulation. *J. Climate*, **21**, 5229–5241, doi: 10.1175/2008JCLI2073.1.

Peters, O., and J. D. Neelin, 2006: Critical phenomena in atmospheric precipitation. *Nature Physics*, **2**, 393–396, doi: 10.1038/nphys314.

Ramage, C. S., 1971: *Monsoon meteorology*. Academic Press, New York, 296 pp.

Raymond, D. J., 1995: Regulation of moist convection over the west Pacific warm pool. *J. Atmos. Sci.*, **52**, 3945–3959, doi: 10.1175/1520-0469(1995)052<3945:ROMCOT>2.0.CO;2.

Raymond, D. J., 2000: Thermodynamic control of tropical rainfall. *Quart. J. Roy. Meteor. Soc.*, **126**, 889–898, doi: 10.1002/qj.49712656406.

Raymond, D. J., and A. M. Blyth, 1986: A stochastic mixing model for nonprecipitating cumulus clouds. *J. Atmos. Sci.*, **43**, 2708–2718, doi: 10.1175/1520-0469(1986)043<2708:ASMMFN>2.0.CO;2.

Raymond, D. J., C. S. Bretherton, and J. Molinari, 2006: Dynamics of the intertropical convergence zone of the east Pacific. *J. Atmos. Sci.*, **63**, 582–597, doi: 10.1175/JAS3642.1.

Raymond, D. J., and Ž. Fuchs, 2007: Convectively coupled gravity and moisture modes in a simple atmospheric model. *Tellus*, **59**A, 627–640, doi: 10.1111/j.1600-0870.2007.00268.x.

Raymond, D. J. and Ž. Fuchs, 2009: Moisture modes and the Madden-Julian oscillation. *J. Climate*, **22**, 3031–3046, doi: 10.1175/2008JCLI2739.1.

Raymond, D. J., G. B. Raga, C. S. Bretherton, J. Molinari, C. Lpez-Carrillo, and Ž. Fuchs, 2003: Convective forcing in the intertropical convergence zone of the eastern Pacific. *J. Atmos. Sci.*, **60**, 2064–2082, doi: 10.1175/1520-0469(2003)060<2064:CFITIC>2.0.CO;2.

Raymond, D. J. and S. L. Sessions, 2007: Evolution of convection during tropical cyclogenesis. *Geophys. Res. Letters*, **34**, L06811, doi: 10.1029/2006GL028607.

Raymond, D. J., S. L. Sessions, and Ž. Fuchs, 2007: A theory for the spinup of tropical depressions. *Quart. J. Roy. Meteor. Soc.*, **133**, 1743–1754, doi: 10.1002/qj.125.

Raymond, D. J., and X. Zeng, 2005: Modelling tropical atmospheric convection in the context of the weak temperature gradient approximation. *Quart. J. Roy. Meteor. Soc.*, **131**, 1301–1320, doi: 10.1256/qj.03.97.

Reed, R. J., D. C. Norquist, and E. E. Recker, 1977: The structure and properties of African wave disturbances as observed during Phase III of GATE. *Mon. Wea. Rev.*, **105**, 317–333, doi: 10.1175/1520-0493(1977)105<0317:TSAPOA>2.0.CO;2.

Reed, R. J., and E. E. Recker, 1971: Structure and properties of synoptic-scale wave disturbances in the equatorial western Pacific. *J. Atmos. Sci.*, **28**, 1117–1133, doi: 10.1175/1520-0469(1971)028<1117:SAPOSS>2.0.CO;2.

Roundy, P. E., and W. M. Frank, 2004: A climatology of waves in the equatorial region. *J. Atmos. Sci.*, **61**, 2105–2132, doi: 10.1175/1520-0469(2004)061<2105:ACOWIT>2.0.CO;2.

Slingo, J. M., et al., 1996: Intraseasonal oscillations in 15 atmospheric general circulation models: Results from an AMIP diagnostic subproject. *Clim. Dyn.*, **12**, 325–357, doi: 10.1007/BF00231106.

Sobel, A. H., 2007: Simple models of ensemble-averaged tropical precipitation and surface wind, given the sea surface temperature. *The Global Circulation of the Atmosphere, T. Schneider and A. H. Sobel Eds*, Princeton University Press, 219–251.

Sobel, A. H., and C. S. Bretherton, 2000: Modeling tropical precipitation in a single column. *J. Climate*, **13**, 4378–4392, doi: 10.1175/1520-0442(2000)013<4378:MTPIAS>2.0.CO;2.

Sobel, A. H., J. Nilsson, and L. M. Polvani, 2001: The weak temperature gradient approximation and balanced tropical moisture waves. *J. Atmos. Sci.*, **58**, 3650–3665, doi: 10.1175/1520-0469(2001)058.

Sobel, A. H., and C. S. Bretherton, 2003: Large-scale waves interacting with deep convection in idealized mesoscale model simulations. *Tellus*, **55**A, 45–60, doi: 10.1034/j.1600-0870.2003.201421.x.

Sobel, A. H., and J. D. Neelin, 2006: The boundary layer contribution to intertropical convergence zones in the quasi-equilibrium tropical circulation model framework. *Theor. Comput. fluid dyn.*, doi: 10.1007/s00162-006-0033-y.

Sobel, A. H., G. Bellon, and J. Bacmeister, 2007: Multiple equilibria in a single-column model of the tropical atmosphere. *Geophys. Res. Letters*, **34**, L22804, doi: 10.1029/2007GL031320

Stephens, G. L., S. van den Heever, and L. Pakula, 2008: Radiative-convective feedbacks in idealized states of radiative-convective equilibrium. *J. Atmos. Sci.*, **65**, 3899–3916, doi: 10.1175/2008JAS2524.1.

Straub, K. H., and G. N. Kiladis, 2002: Observations of a convectively coupled Kelvin wave in the eastern Pacific ITCZ. *J. Atmos. Sci.*, **59**, 30–53, doi: 10.1175/1520-0469(2002)059<0030:OOACCK>2.0.CO;2.

Sugiyama, M., 2009: Moisture mode in the tropics. Part I: Analysis based on the weak temperature gradient approximation. *J. Atmos. Sci.*, **66**, 1507–1523, doi: 10.1175/2008JAS2690.1.

Tompkins, A. M., 2001: Organization of tropical convection in low vertical wind shears: The role of water vapor. *J. Atmos. Sci.*, **58**, 529–545, doi: 10.1175/1520-0469(2001)058<0529:OOTCIL>2.0.CO;2.

Tulich, S. N., D. A. Randall, and B. E. Mapes, 2007: Vertical-mode and cloud decomposition of large-scale convectively coupled gravity waves in a two-dimensional cloudresolving model. *J. Atmos. Sci.*, **64**, 1210–1229, doi: 10.1175/JAS3884.1.

Webster, P. J., and R. Lukas, 1992: TOGA COARE: The TOGA coupled ocean-atmosphere response experiment. *Bull. Am. Meteor. Soc.*, **73**, 1377–1416, doi: 10.1175/1520-0477(1992)073<1377:TCTCOR>2.0.CO;2.

Williams, E. R., S. A. Rutledge, S. G. Geotis, N. Renno, E. Rasmussen, and T. Rickenbach, 1992: A radar and electrical study of tropical "hot towers". *J. Atmos. Sci.*, **49**, 1386–1395, doi: 10.1175/1520-0469(1992)049<1386:ARAESO>2.0.CO;2.

Yano, J.-I., and K. Emanuel, 1991: An improved model of the equatorial troposphere and its coupling with the stratosphere. *J. Atmos. Sci.*, **48**, 377–389, doi: 10.1175/1520-0469(1991)048<0377:AIMOTE>2.0.CO;2.

Yu, J.-Y., and J. D. Neelin, 1994: Modes of tropical variability under convective adjustment and the Madden-Julian oscillation. Part II: Numerical results. *J. Atmos. Sci.*, **51**, 1895–1914, doi: 10.1175/1520-0469(1994)051<1895:MOTVUC>2.0.CO;2.

Yu, J.-Y., and J. D. Neelin, 1997: Analytic approximations for moist convectively adjusted regions. *J. Atmos. Sci.*, **54**, 1054–1063, doi: 10.1175/1520-0469(1997)054<1054:AAFMCA>2.0.CO;2.

Yu, J.-Y., C. Chou, and J. D. Neelin, 1998: Estimating the gross moist stability of the tropical atmosphere. *J. Atmos. Sci.*, **55**, 1354–1372, doi: 10.1175/1520-0469(1998)055<1354:ETGMSO>2.0.CO;2.

Zeng, N., J. D. Neelin, and C. Chou, 2000: A quasi-equilibrium tropical circulation model – implementation and simulation. *J. Atmos. Sci.*, **57**, 1767–1796, doi: 10.1175/1520-0469(2000)057<1767:AQETCM>2.0.CO;2.

Zhang, C., B. E. Mapes, and B. J. Soden, 2003: Bimodality in tropical water vapour. *Quart. J. Roy. Meteor. Soc.*, **129**, 2847–2866, doi: 10.1256/qj.02.166.

Zhang, C., 2005: Madden-Julian oscillation. *Rev. Geophys.*, **43**, doi: 10.1029/2004RG000158.

Zhang, C., M. McGauley, and N. A. Bond, 2004: Shallow meridional circulation in the tropical eastern Pacific. *J. Climate*, **17**, 133–139, doi: 10.1175/1520-0442(2004)017<0133:SMCITT>2.0.CO;2.